EROGRASS

Failure of Grass Cover Layers at Seaward and Shoreward Dike Slopes

- Design, Construction & Performance -

April 2009

Report	**EroGRASS** **Failure of Grass Cover Layers at Seaward and Shoreward Dike Slopes** - Design, Construction and Performance -
Lead Author	Thorsten Piontkowitz
Contributors	Henk Jan Verhagen, Henk Verheij, Tri Mai Cao, Darshana Dassanayake, Dano Roelvink, Stefano Utili, Marcin Zielinski, Are Kont, Tõnu Ploompuu
Distribution	Partners EroGRASS, Coastal Research Centre (GWK)
Citation	Piontkowitz, T.; Verhagen, H.J.; Verheij, H.; Mai Cao, T.; Dassanayake, D.; Roelvink, D.; Utili, S.; Zielinski, M.; Kont, A.; Ploompuu, T. (2009): EroGRASS - Failure of Grass Cover Layers at Seaward and Shoreward Dike Slopes. Design, Construction and Performance. EroGRASS User Group. Lemvig (Denmark), pp. xx.

Acknowledgement

The work described in this publication has been supported by the 6th EC Framework Programme through the Integrated Infrastructure Initiative HYDRALAB III.

For additional information on the EroGRASS project please visit: www.kyst.dk/erograss.

Keywords

Grass cover failure, wave impact, run up and run down flows, wave overtopping, grass sods, prototype dike model, Large Wave Chanel.

Summary

A large number of the dikes in the North Sea and Baltic Sea regions are covered with grass that is exposed to hydraulic loading from waves and currents during storm surges. During previous storm surges the grass cover layers often showed large strength and remained undamaged. A clear physical understanding of the failure of grass cover layers due to different wave loads is therefore indispensable today, especially against the background of enhanced hydraulic impact due to climate change.

The strength of the grass cover layer lies mainly in its ability to withstand three types of wave actions:

- Wave impact due to wave breaking on the seaward slope
- Wave run-up and run-down flow after wave breaking on the seaward slope
- Down-slope flow on the landward slope caused by wave overtopping.

The main objectives of this research project are therefore to perform large scale model tests to investigate in detail the failure of grass cover layers due to (i) wave impact, (ii) wave run-up and run-down flow and (iii) wave overtopping.

Wave impact as well as wave run-up and run-down flow may induce grass cover failure on the seaward dike slope. Wave overtopping causes failure of the grass cover at the dike crest and on the shoreward slope. Hence, this research project deals with the investigation of grass cover failure anywhere along a dike profile: seaward slope, dike crest and shoreward slope. It is envisaged that the proposed research and tests will improve the understanding of the failure of grass cover layers due to wave loading.

To obtain the aforementioned research objectives, large scale model tests at a dike model have been performed in the Large Wave Flume of the Coastal Research Centre – a joint centre of the University of Hanover and the Technical University of Braunschweig, Germany. The dike model represents a typical sea dike. With exception of the seaward slope, it is comparable to typical cross sections of sea dikes built in The Netherlands, Germany and Denmark. This relatively steep seaward slope has been chosen to improve the generation of wave impact on the seaward slope. The crest height of the dike model is 5.8m above the bottom of the wave flume and the dike model consists of a sand core covered by a layer of clay and a grass layer. The 0.2m thick grass cover layer is constructed with grass sods that have been excavated at the existing Ribe sea defence in Denmark and transported to the Large Wave Channel in Hannover by trucks.

The report presents a first reporting of the EroGRASS project including a description of the design and construction of the dike model in the Large Wave Flume, the measuring and observation techniques and the test programme together with examples of records from the performed tests. Focus of this report is put on providing a well-documented description of the aforementioned issues, whereas the data analysis and presentation of the results are not included in this report since these are in progress and will be reported later.

Contents

1. Introduction

Along the North Sea coasts, coastal flood defence is mainly performed by dikes. Grass cover layers on the seaward and shoreward slopes are the most prevalent form to protect the dike surface against erosion during storm surges. The grass cover layer is then exposed to different forms of wave loading that may provoke the failure of the grass cover. As the failure of the grass cover layer may emerge to an overall dike breach, the clear understanding of the failure processes is essential for estimating the safety of a sea dike. The main objectives of the EroGRASS project have therefore been to perform large scale model tests to investigate in detail the failure of grass cover layers due to (i) wave impact, (ii) wave run-up and run-down flow and (iii) wave overtopping. The large scale tests at a prototype dike model were performed in the Large Wave Flume (GWK) of the Coastal Research Center (a joint centre of the Universities of Hannover and Braunschweig) in Hannover, Germany.

The report in hand is a first reporting of the EroGRASS project containing a description of the design and construction of the dike model in the Large Wave Flume, the measuring and observation techniques and the test programme together with examples of records from the performed tests. Focus of this report is put on providing a well-documented description of the aforementioned issues, whereas the data analysis and presentation of the results are not included in this report since these are in progress and will be reported later.

1.1 State of knowledge

According to Young (2005), the assessment of the grass cover being exposed to these hydraulic loadings involves three distinct scientific or engineering disciplines:

- Hydraulics – wave loading;
- Geotechnics – strength of the soil structure (shear strength and erodibility of the clay layer);
- Botany – composition, management and strength of the grass cover layer.

The structure and division of a grass cover is shown in Figure 1.1. The green leafy part of the grass is the sward. The turf is the root mat which provides the strength and erosion resistance to the cay layer. The roots keep the soil particles together and create a flexible and tough layer that offers significantly higher erosion resistance than a bare clay layer (Young, 2005). Model tests by Möller et al. (2002) showed that as soon as water is flowing over a bare clay surface, gulley formation will start rapidly.

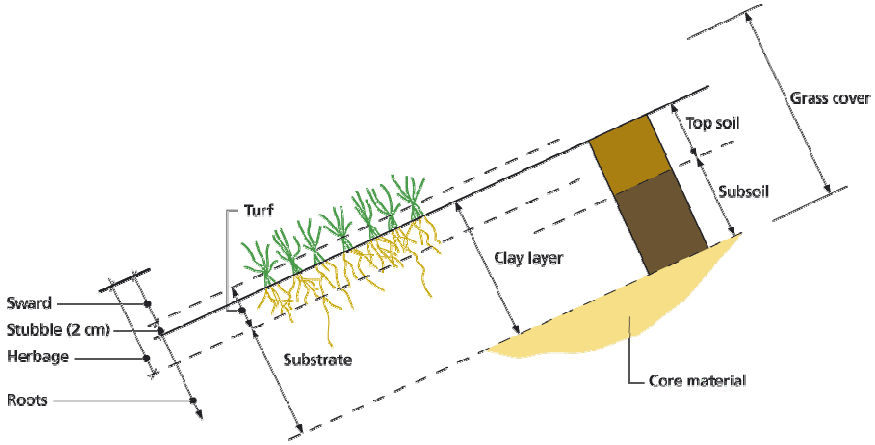

Figure 1.1 Structure and division of a grass cover (TAW, 1997).

Investigations carried out by Sprangers (1999) show that the performance of grassland depends primarily on its management. The ideal grassland is unfertilised, periodically grazed and rich of species. This form of management provokes a closed turf with fine and coarse roots. This network of fine and coarse roots makes the top soil a strong and flexible layer that can deform without tearing (TAW, 1997). Hence, the root network is important to keep the clay particles together during wave loading. The TAW (1997) states further that the structure of the soil in between the roots is at least as important. Both aspects are the most important characteristics for erosion resistance of the grass cover at sea dikes during wave loading.

At the same time as grass turf establishes, so the clay properties changes. The moisture content changes leading to shrinkage and shear cracks in the clay. The change of the moisture content is due to the plant extraction of water from the clay. The soil cracking produces a soil that consists of aggregates of various dimensions. The composition of these cracks and aggregates, together with pores and aggregates made by animals, is called the soil structure (TAW, 1996).

According to TAW (1996), the soil structure may be present to a depth of more than 0.8 m. The soil cracking increases the permeability of the soil and the infiltration of water into the subsoil. Infiltration tests at many locations on dikes resulted in infiltration rates of 10-5 to 10-4 m/s (TAW, 1996). The infiltration of water into the clay layer can induce the loosening of individual particles, which may lead quickly to major damage of dike construction. In the case of a sandy clay (> 40%), the erosion of the soil may appear even more faster. Hence, the erosion of clay depends on the water content and the sand content. The erosion resistance may be classified into three categories (TAW, 1996):

Table 1.1 Classification of clay erosion resistance (TAW, 1996).

Category	Water content w [%]	Plasticity index I_p	Sand content [%]
Erosion-resistant clay	> 45	> 0.73 · (w - 20)	< 40
Moderately erosion resistant clay	< 45	> 18	< 40
Clay with little erosion resistance	< 45	< 18	> 40

Several large scale tests have been performed to improve the knowledge about the strength of dike grassland. Young (2005) reports about two physical tests performed in the Netherlands: (i) the Deltagoot test in 1992 and (ii) the Scheldbak test in 1994. At these tests attention was paid on the vegetation quality and soil quality. The aspect of hydraulic loading received less attention.

Since flood defence system management changes recently to more reliability and risk-based design concepts, the clear physical understanding of grass erosion due to different forms of wave loading has gotten more important. The overall goal is to produce a set of limit state equations (Young, 2005) that predict the failure of the grass cover due to wave loading (wave run-up and run-down flow, wave impact, wave overtopping).

Preliminary theoretical investigations with respect to wave overtopping flow on inner slopes have been undertaken by IHE Delft. Based on a comprehensive literature review, Young (2005) questions the relevance of surface erosion as a failure mode and states that surface erosion may not be the sole mechanism of grass cover failure on inner dike slopes. He suggests a superficial slip model that looks at the shear failure at the interface between the

turf and clay layer. The sliding mechanism presumes a condition of full saturation, and seepage parallel to the surface (Young, 2005).

In the case of the top layer being dominated by soil structure, Young (2005) argues further, that the soil (without grass) will not exhibit cohesion. Since turf is a composite material including roots, quantities such as root tensile strength and root area ratio are introduced to quantify the additional strength from roots. Concerning root tensile strength, the literature review by Young (2005) showed that more should be know about the range or distribution of root diameters for dike grassland, before root tensile strength can be quantified. Direct tensile strength tests on the roots of dike grassland have not been performed yet (Young, 2005).

The root area ratio can be back-calculated from root mass, root length and cross section area. Referring to measured profiles by Simon and Collison (2001) and root measurements by Sprangers (1999), Young (2005) states that the root area decreases with depth. The root measurements by Sprangers (1999) showed that 53-55% of the roots are located in the top 6 cm of the turf, and that 75-80% of the roots is within the top 20 cm.

Theoretical investigations for wave impact or wave run-up (seaward slope), comparable to the review for wave overtopping by Young (2005), could not be found in the literature.

1.2 Motivation and objectives

In recent years, the interest of reliability and risk-based design concepts has grown clearly in the field of coastal engineering. At this, the clear physical understanding of load-resistance processes has become an essential task. At the same time, grass cover layers as revetments for flood defence structures have attracted more interest. A grass cover is now being considered as a constructional component (EAK, 2002) that has to be designed and managed.

Design and management of grass cover layers require an improved understanding of the failure development and the interaction between load and resistance. The problem of erosion at dike slopes and crests during wave loading appears here to be critical. Young (2005) indicated the loads which may cause erosion of the grass cover layer at sea dikes, namely:

- Overflow (still water level exceeds the crest level)
- Wave impact due to wave breaking on the seaward slope
- Wave run-up and run-down flow on the seaward slope
- Flow on the shoreward slope due to wave overtopping

The clear physical understanding of the failure of grass cover layers due to these different forms of wave loading is however indispensable today, especially against the background of enhanced focus on risk-based design methods and sustainable management strategies of coastal flood defences (e.g. sea dikes).

The main objectives of this research project are therefore to perform large scale model tests to investigate in detail the failure of grass cover layers due to (i) wave impact, (ii) wave run-up and run-down flow and (iii) wave overtopping. The loading by overflow will not be considered.

Wave impact as well as wave run-up and run-down flow may induce grass cover failure on the seaward dike slope. Wave overtopping causes failure of the grass cover at the dike crest and on the shoreward slope. Hence, this research project deals with the investigation of grass cover failure anywhere along a dike profile: seaward slope, dike crest and shoreward slope. It is envisaged that the proposed research and tests will improve the understanding of the failure of grass cover layers due to wave loading.

To obtain the aforementioned research objectives, large scale model tests have been performed in the Large Wave Flume of the Coastal Research Centre – a joint centre of the University of Hanover and the Technical University of Braunschweig, Germany.

2. Design of the dike model

The prototype of the selected dike model represents a typical sea dike of the German Bight coast (Figure 2.1). With exception of the relatively steep seaward slope, it is comparable to typical dike cross sections as commonly built in The Netherlands, Germany and Denmark. Generally sea dike consists of a sand core, a clay layer and a grass cover. According to EAK (2002), landward dike slopes are build 1:3 and seaward dike slopes are recommended not steeper than 1:6. In prototype the crest of the sea dike can be 3m wide and the height of the sea dike can be 8.4m or more. The seaward and the landward slopes are normally constructed without berms to ease the construction of the sea dike (Oumeraci et al., 2001a).

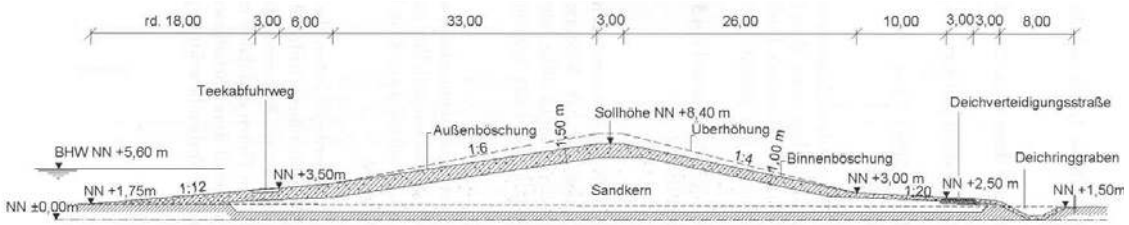

Figure 2.1 Typical cross-section of a grass-covered sea dike at the German Bight coast (EAK, 2002).

2.1 Geometry of the model

The Large Wave Flume (GWK) of the Coastal Research Centre in Hannover (Germany) is 5m wide, 7m deep and 324m long (Figure 6). The maximum water depth in the flume is 5.0m. Regular waves can be generated with heights up to H ≈ 2.50m and irregular waves with significant heights up to Hs ≈ 1.5m. The prototype of the dike model was therefore adjusted in its dimensions and geometry to allow for large scale testing in the wave flume.

2.1.1 Cross section

Changes in comparison to a prototype were made concerning the dike height and seaward slope. The slope of the seaward side was chosen to 1:4. This relatively steep slope was preferred instead of 1:6 in order to investigate breaking wave impact loads on the seaward slope without the damping effect of the water layer of the previous wave down rush. The landward slope was 1:3. The height of the dike model was 5.8m and the crest was 2.2m wide (Figure 2.2). No berms were constructed on both slopes. The length of the dike model was 5m like the width of the flume.

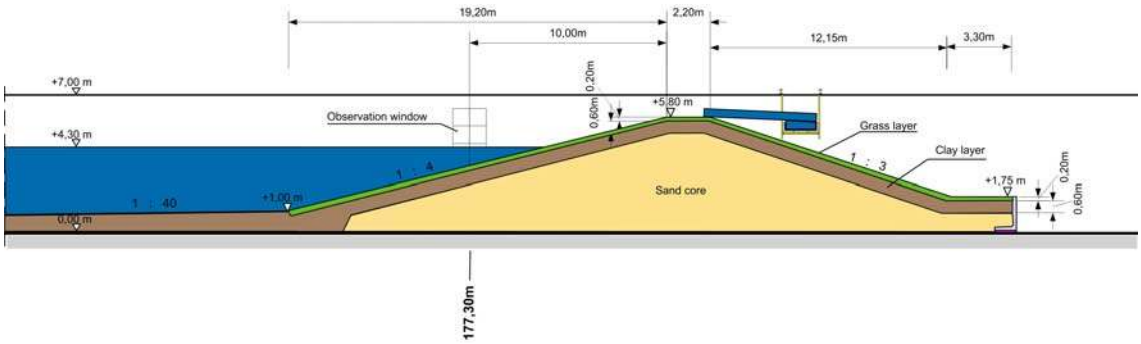

Figure 2.2 Cross section of the dike model.

The dike model consisted of a sand dike core, a clay layer and a grass cover. On both slopes and on the dike crest a clay layer of 0.6m was installed. On top of the clay layer, 0.2m thick grass sods were placed to complete the dike model with a grass cover layer. Through this, the entire clay layer was about 0.8m thick.

In front of the dike model a sloping foreshore was installed to ensure proper conditions for the development of waves (shoaling) in front of the dike model. The slope of the foreshore was 1:40 and the height at the dike toe was 1.0m above the flume bottom. The foreshore length was 40m.

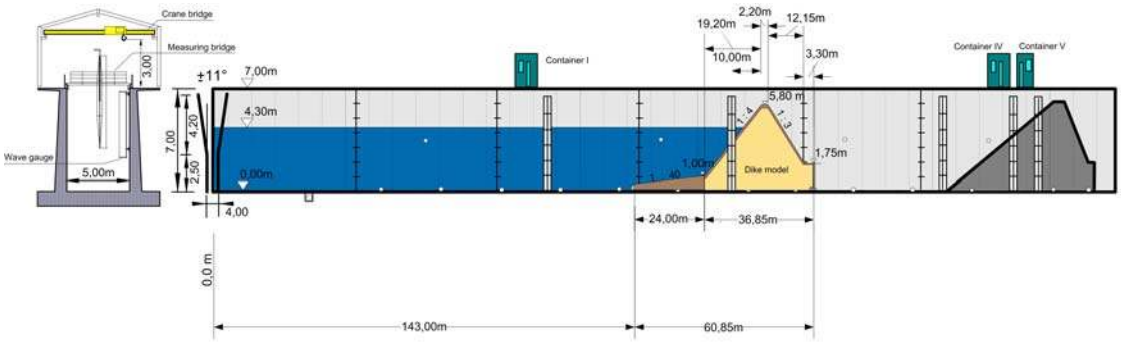

Figure 2.3 Cross and longitudinal section of the Large Wave Flume (Hannover) showing the positioning of the dike model in the flume.

The combined inlet and outlet of the flume is about 35m from the wave paddle. The model was located about 190m from the wave generator because there is a window which enables to observe the influence of breaking waves on the seaward slope of the dike model (Figure 2.3). The flume area behind the dike model was needed as a reservoir for wave overtopping.

2.1.2 Dike toes and transition to flume bottom

The transition between the seaward dike toe and the foreshore is shown in Figure 2.4. The foreshore was built of clay that was connected with the clay layer of the seaward dike slope in order to perform a sealing against infiltrating water (Detail A, Figure 2.6).

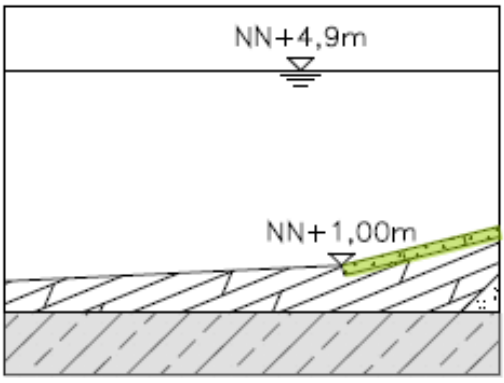

Figure 2.4 Detail A – Transition between dike toe and foreshore (see Figure 2.6).

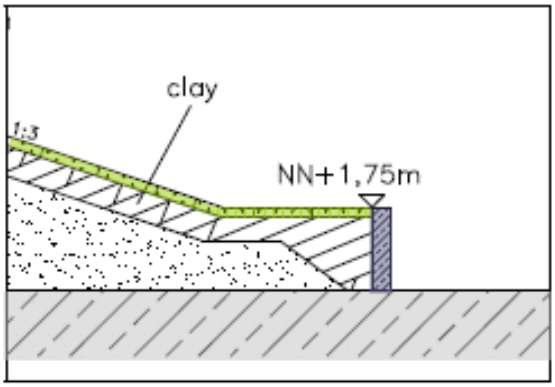

Figure 2.5 Detail B –Toe protection of the landward slope (see Figure 2.6)

The toe of the landward slope is stabilised by a concrete corner wall (Detail B, Figure 2.6). In front of the concrete wall the clay is build in down to the flume bottom (Figure 2.5). The concrete wall is required to avoid a head cut erosion of the landward dike toe.

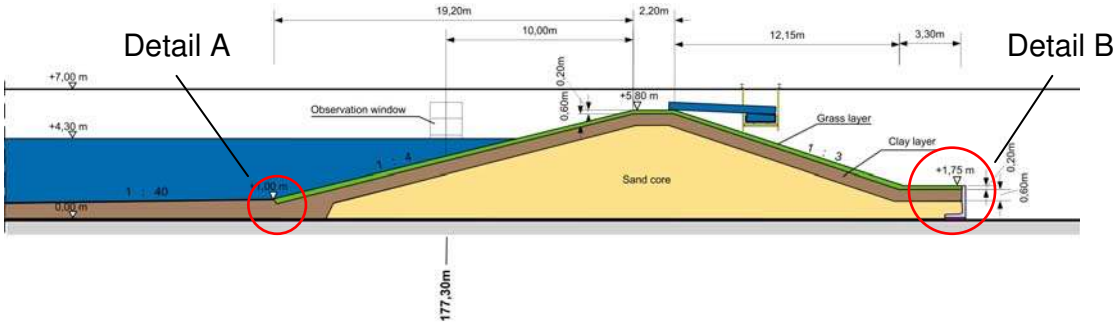

Figure 2.6 Cross section of the dike model showing the construction details A and B.

With the 0.8m thick clay layer and both construction details A and B, the sand core is completely covered by clay and infiltration into the sand core is reduced. To avoid piping as well as pore pressure build up and seepage, the dike body was drained. The drainage decreases the water content in the dike core. The drainage system was located on the flume bottom and was emptied by a pump. The phreatic water was pumped into the reservoir behind the dike model.

2.2 Construction materials

To fulfil the objectives of this research project, the dike model had to be covered with a natural grass layer. The challenge was hereby to get the natural grass into the flume. Since it was not feasible to sow grass on the clay layer and wait for a well-established grass cover, grass sods had to be excavated from an existing sea dike and transported to the wave flume for installation on the dike model.

The flood defence system from where the grass sods were excavated is shown in Figure 2.7. The grass cover originated from the flood defence system near Ribe (Denmark). The grass sods were excavated from the southern wing dike which was reinforced in 1998. The composition of grass community of the southern wing dike is very similar to those used in Germany and the Netherlands.

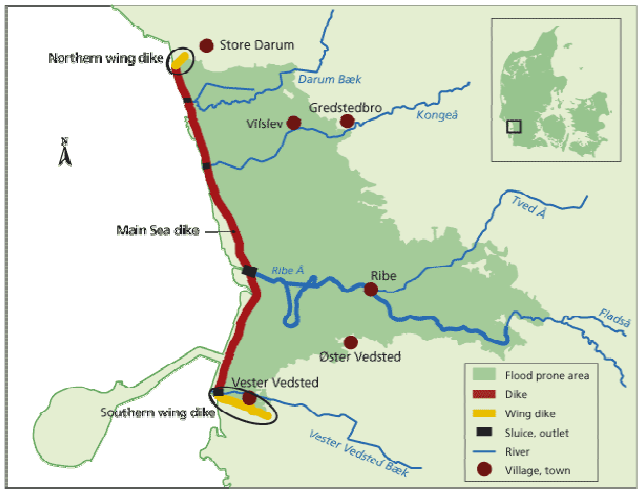

Figure 2.7 Location of the Ribe defence system and its wing dikes (Denmark).

The grass sods were excavated with the underlying clay, as it was important that the interaction between the grass layer (top soil) and the underlying clay layer was not disturbed. The grass was of good quality and adequate for investigation of incipient erosion of the grass cover.

The complete dike surface to be covered with grass was calculated to about 190m^2. An area of about 10m^2 of grass sods were estimated for substitution of damaged grass areas during testing. In total, about 200m^2 of grass sods were therefore excavated. The cross section of an excavated grass sod is shown in Figure 2.8. The excavated grass sods were about 20cm thick and measured 2.35m in length and 1.25m in width. The weight of one grass sod was determined to approximately 1,100 kg.

In order to cover the dike model with a 0.6m thick clay layer, a total clay volume of about 150m^3 was needed. Furthermore, a volume of 5m^3 was estimated to repair damaged parts of the dike model.

Figure 2.8 Cross section of a 20cm thick excavated grass sod.

A sand volume of 300m^3 was needed to construct the dike core. The sand was available at the Coastal Research Centre. The medium diameter was determined d_{50} = 0.33mm. This grain size is slightly larger than the typical sand material used for dike cores at prototype. Table 2.1 lists all needed materials for construction of the dike model.

Table 2.1 Needed material for construction of the dike model.

Type	Area / Volume	Quality / Type	Taken from
Grass	~ 200 m^2	Winter grass	Sea defence system at Ribe, Denmark
Clay	~ 150 m^3	Good	Sea defence system at Ribe, Denmark
Sand	~ 300 m^3	D_{50} = 0.33mm	Available at CRC

2.2.1 Sand for the dike core

The dike core consisted of sand with 70% of the sand grains being smaller than 0.25mm (Figure 2.9). The EAK (2002) recommends a percentage of fine particles (d ≤ 0.063mm) not higher than 15% and the compaction level should range within 90-98% of maximum proctor density.

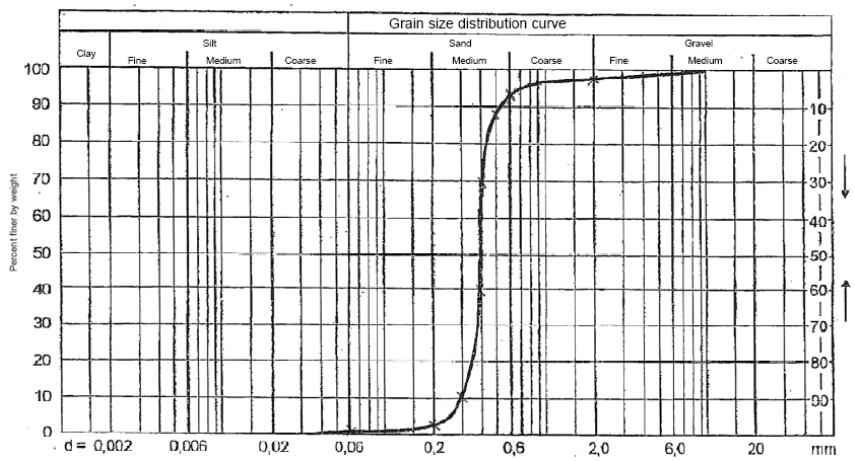

Figure 2.9 Grain distribution curve of the sand used for dike core construction in the Large Wave Flume.

2.2.2 Clay for the dike revetment

The erosion resistance of clay can be categorised by the water content and the sand content. Clay can be classified into three erosion resistant categories according to TAW (1996), see Table 2.2. According to EAK (2002), clay which is used for sea dike revetments should also meat the requirements specified in Table 2.3.

Table 2.2 Classification of clay erosion resistance (TAW, 1996).

Clay category	Water content w [%]	Plastic index	Sand content [%]
Erosion resistant	> 45	> 0.73 · (w - 20)	< 40
Moderate erosion resistance	< 45	> 18	< 40
Low erosion resistance	< 45	< 18	< 40

Table 2.3 Requirements for clay used as dike revetment (EAK, 2002).

Soil property	Threshold
Sand content (d > 0.06mm)	< 40%
Clay content (d < 0.002mm)	> 10%
Liquidity limit	w_L > 25%
Plasticity limit	w_P > 15%
Undrained soil cohesion	C_u > 20 KN/m2
Dry density	0.85 < ρ_d < 1.45 t/m^3
Water content	80% > w > 30%

The soil properties of the clay used for the clay revetment of the dike model (Type B, Table 2.4) were determined by Strathclyde University using the geotechnical laboratory at Leichtweiß-Institute. The soil properties of the clay used for the foreland (Type A, Table 2.4) had been determined in a former project by Richwien & Weißmann (2001). The grain size distribution of clay type A and clay type B are shown in Figure 2.10. For both clay types accounts that the soil properties were determined according to the German standards DIN 18121, 18122, 18123 and 18137.

Table 2.4 Soil properties of the clay used for the dike model.

Soil property	Clay – Type A Foreshore	Clay – Type B Clay revetment
Sand content (d > 0.06mm)	12%	20%
Clay content (d < 0.002mm)	35%	25%
Liquidity limit w_L	77%	61%
Plasticity limit w_P	45%	28%
Dry density	1.612 t/m^3	1.373 t/m^3
Water content	40% - 50%	26% - 35%

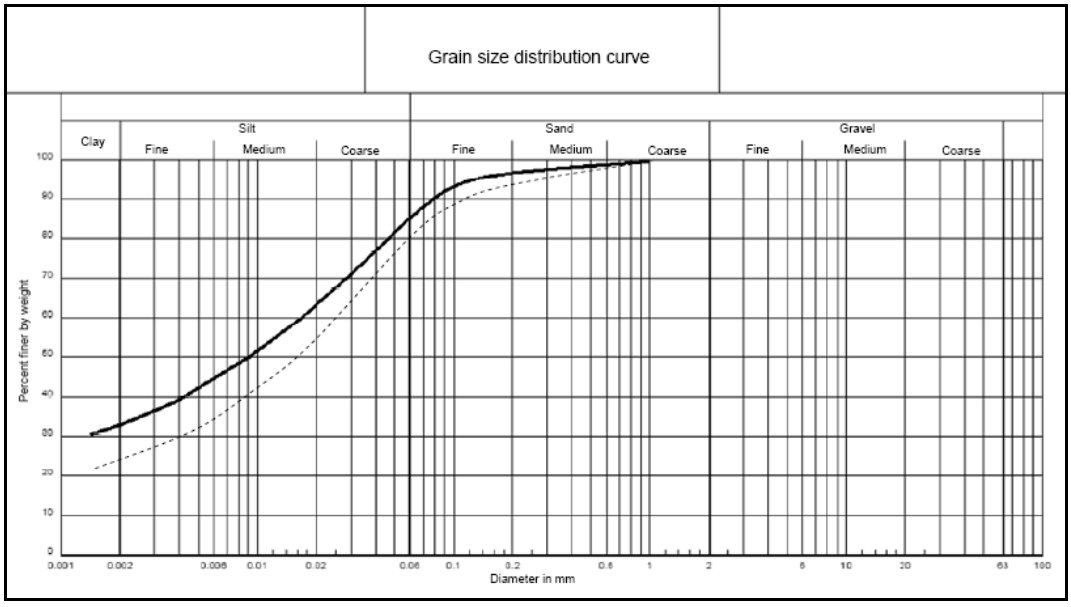

Figure 2.10 Grain size distribution of clay type A (continuous line) and clay type B (dashed line).

2.2.3 Grass cover

The grass cover consists of grass vegetation (grass field) rooted in the underlying soil (clay) (Figure 2.11). A good resistant grass cover consists of a high number of species (TAW, 1999).

The soil near the surface of the top layer has a high root density, is elastic in moist conditions and porous. Conversely, the underlying clay is stiff (or plastic when moist or not yet aged) and usually somewhat less permeable. The erosion resistance of the covering layer, near the soil surface, is (usually) greater than at deeper parts of the layer. The upper, densely rooted

part, with an irregular bed structure and a higher erosion resistance, is called sod. Sod with a thick network of roots and a coverage of grass higher than 70-85% has a good erosion resistance. 65% of the grass roots are located in the upper soil layer (0-6cm depth). Between 6cm and 15cm 20% of the roots can be found. The rest of roots are located in a depth up to 50cm (Sprangers, 1999).

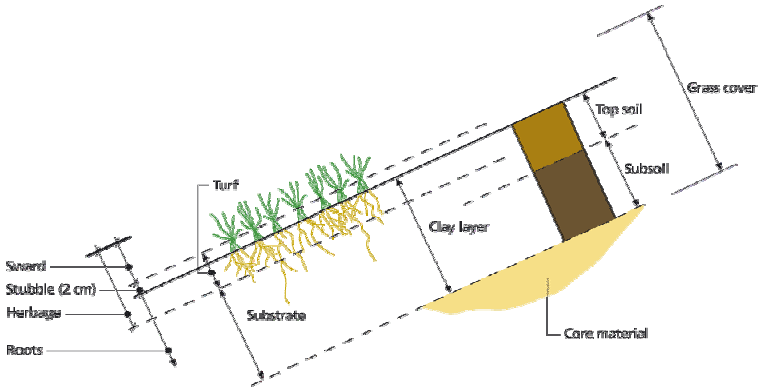

Figure 2.11 Structure of the clay and grass cover used for the dike model.

The degree of prevention of high velocities and stresses at the soil-water interface of vegetal cover is described by the vegetal cover factor C_F, see Temple et al. (1987). The cover factor is dominated by the density and uniformity of density in the immediate vicinity of the soil boundary. In Table 2.5 generalised vegetal cover factors are shown. These do not depend on the species of the vegetal cover.

Table 2.5 Vegetal cover factor by Temple & Hanson (1994).

Cover description	Vegetal cover factor C_F
Good vegetal cover	0.75
Fair vegetal cover	0.50
Poor vegetal cover	0.25

The vegetal cover factor can be specified by different species. The species of the cover influence the vegetal cover factor. The vegetal cover factors for different species are given in Table 2.6.

Table 2.6 Properties of different grass species[1] (Temple et al., 1987).

Grass	Cover factor C_F	Reference stem density (Stem/m^2)
Bermudagrass Centipedegrass	0.90	5400 5400
Buffalograss Blue grama	0.87	4300 3800
Grass mixture	0.75	2200

[1] The stem density has to be multiplied with 1/3, 2/3 and 1 for poor, fair and good grass cover condition.

From large-scale tests performed in the Deltagoot (Netherlands) in 1992 (Smith et al. (1994)) a conservative classification for the determination of the erosion resistance of grassland against wave impact on the seaward side is given in Table 2.7.

Table 2.7 Grass erosion coefficient (TAW, 1997).

Erosion-resistant grassland	Expected values for c_E
Good	0.5 to 1.5 10^{-6} $(ms)^{-1}$
Moderate	1.5 to 2.5 10^{-6} $(ms)^{-1}$
Poor	2.5 to 3.5 10^{-6} $(ms)^{-1}$

The typical grass species and their fraction generally found in the grass cover of sea dikes are listed in Table 2.8.

Table 2.8 Typical grass species and fraction on sea dike.

Grass species		Sort	Portion
Latin	*English*		
Festuca arundinacea	Tall fescue	Fine Lawn	20%
Festuca rubra	Red fescue	Suzette S	20%
Festuca rubra	Red fescue	Echo	40%
Lolium hybridum	Hybrid ryegrass	Avance	15%
Agrostis stolonifera	Creeping wheat	Kromi S	2.5%
Agrostis capillaris	Browntop	Highland bent.	2.5%

Root volume ratio (RVR)

The influence of the root network on the reinforced soil strength can be investigated by determining the root percentage in the soil sample. For the dike model the Root Volume Ratio (RVR) was determined at the Leichtweiß-Institute by using the following procedure:

Soil samples were taken from different grass sods. Each sample block measured 10cm x 10cm x 20cm. The part above the soil surface of each grass block was removed including the lose material on the surface. The block was then cut into 2cm thick slices with an area of 10x10cm. The volume of each slice was 200cm^3. Each slice was carefully washed and the roots were collected. After drying the roots at a temperature of 105°C for 24 hours, they were weighted. Young (2005) suggests that the grass root density is estimated with 300kg/m^3. The volume of the entire roots of a slice was determined in relation to the slice volume. In total, six sample blocks were analysed and the root volume ratio (RVR) was determined (Figure 2.12).

The information about the grass root distribution is of crucial importance for the estimation of the reinforcement effect of the grass roots on the clay layer. The logarithmic decline of the root volume ratio with increasing depth corresponds with the root volume ratio of ten soil samples analysed by Stanczak (2008).

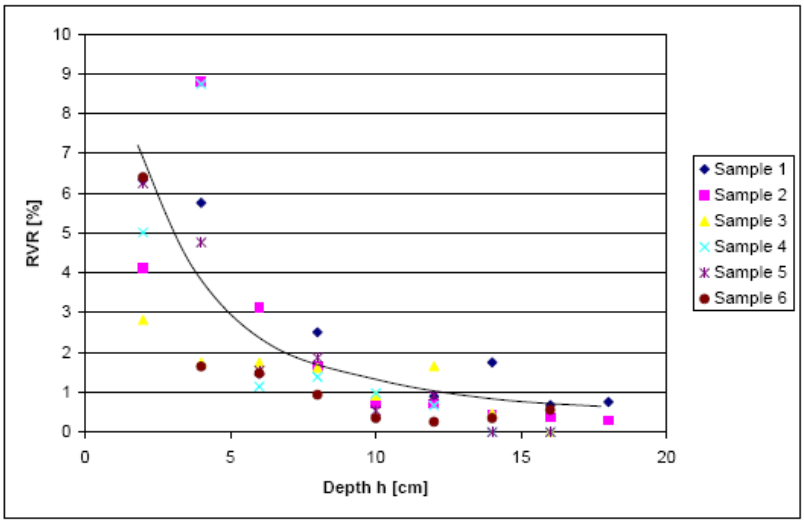

Figure 2.12 Root volume ratio (RVR) of the grass cover used for the dike model.

3. Construction of the dike model

The construction of the entire dike model took about six weeks lasting from 14 January 2008 to 7 March 2008. Construction of the dike model started with installation of the foreshore. The sand core including the drainage system was constructed afterwards, followed by the 60cm thick clay layer which was installed on top of the sand core. After compaction of the clay the 20cm thick grass sods were installed.

3.1 Construction of sand core and foreshore

The construction of the dike model started with installation of the foreshore (Figure 3.1). The compaction density of the applied clay was measured several times during installation and ranged between 1.52 and 1.612t/m³ with a moisture content of about 22.0% and 22.8%. The applied foreshore clay (Type A) was different to the clay (Type B) which was used for the clay layer at the dike model (cp. Table 2.4). The clay for the foreshore (Type A) was available at the Large Wave Flume. The toe of the foreshore was protected by three 1.33m long and 40cm high concrete blocks to avoid erosion of the foreshore toe (Figure 3.1).

After installation of the foreshore, the lower part of the sand core was heaped up. However, before that, the required drainage system was installed. The system consisted of three pipes (diameter of 20cm) wrapped with coco fibres (Figure 3.2). All three pipes ran into a well on the landward side behind the dike model.

Figure 3.1 Foreshore with toe protection (view from sea side).

Figure 3.2 Drainage system installed at the flume bottom.

The well was constructed after the sand core and clay layer of the dike model had been constructed, as it was located just behind the concrete wall of the landward side. The well consisted of three prefabricated concrete rings. It was calked against water intrusion from outside (Figure 3.3).

Figure 3.3 Well and toe on the landward side of the dike model.

The final foreshore is shown in Figure 3.4. The sand of the dike core was transported by a wheel loader (Figure 3.5) from the sand storage into the flume. The sand storage was located on the same yard as the flume. The sand was installed in 50cm thick layers (Figure 3.6) which were afterwards compacted by a plate compactor. Due to only one entree into the flume, the installation of the clay layer on the seaward slope was started simultaneously during construction of the upper sand core layers (Figure 3.7).

Figure 3.4 Final foreshore with clay depot for the seaward clay revetment.

Figure 3.5 Drainage system installed at the flume bottum.

Figure 3.6 Lower part of the sand core. Dike profile is drawn on the flume wall.

Figure 3.7 Simultaneous construction of the seaward clay layer on the dike model.

3.2 Construction of the clay layer

As mentioned before, clay material for the dike model was dug at a clay pit near the harbour town of Esbjerg (Denmark). The clay was transported by trucks from Denmark to Hannover (Figure 3.8) and was stored shortly on the yard of the Coastal Research Centre. (Figure 3.9).

The clay was transported by the wheel loader into the flume. First the lower part of the clay layer on the seaward slope was installed (Figure 3.10). The entire clay layer of 60cm thickness was build in two steps, each time installing a 30cm thick layer with subsequent compaction of the clay material. After construction of the seaward clay layer and finishing of the complete sand core, the clay layer on the landward slope as well as on the crest was installed (Figure 3.11). Clay compaction between two 30cm thick clay layers was performed by a loader (Figure 3.12). After installation of the second 30cm thick clay layer, the clay material was compacted using a rammer and a small roll (Figure 3.13).

Figure 3.8 Unloading of the clay at the yard of the Coastal Research Centre.

Figure 3.9 Temporary stored clay at the yard of the Coastal Research Centre.

Figure 3.10 Lower part of the seaward clay layer.

Figure 3.11 Clay layer on the landward dike slope.

Figure 3.12 Loader used in the Large wave Flume.

Figure 3.13 Clay compaction with a roller.

3.3 Excavation of the grass sods

During the last week of January 2008 the grass sods were excavated from the dike crest of the southern wing dike near Ribe (Denmark). Excavation of the 80 grass sods lasted 3 days. The size of one grass sod was 2.35m in length and 1.25m in width. The thickness of the grass sods varied from 17cm to 22cm.

In detail, a tractor was equipped with an attachment composed of one horizontal blade and two smaller vertical blades. The cutting width of the horizontal blade measured 1.25m. The attachment was assigned to cut the grass sod underneath and at both sides (Figure 3.14). While pulling the attachment, a wooden plate connected with two chains to the attachment was pulled underneath the grass sod. The wooden plate measured 2.35m in length, 1.25m in width and was 25mm thick.

Figure 3.14 Attachment with blades to cut the grass sods.

Figure 3.15 Lifting the grass sod on the wooden plate with a fork lifter.

After the wooden plate was pulled under the grass sod, the cutting process was stopped and the fork of a fork lifter was pushed under the wooden plate to lift up the plate and the grass sod (Figure 3.15). Then the edges of the grass sod were cut straight by hand (Figure 3.16) and the grass sod was driven from the dike crest down to an adjacent field for further action (Figure 3.17). This procedure was used for all 80 grass sods.

Figure 3.16 Attachment with blades to cut the grass sods.

Figure 3.17 Temporary storage of the excavated grass sods on an adjacent field.

Figure 3.18 Installation of four wooden beams for further handling of the grass sods.

Figure 3.19 Construction of wooden frames around each grass sod.

For further handling and transportation four wooden beams were installed under the plate (Figure 3.18) and a wooden frame was built around the sod to avoid any damage or the appearances of additional fissures (Figure 3.19). All grass sods were stored on the field close to the wing dike for 1-3 days before the transport to Hannover started.

3.4 Installation of the grass sods

After unloading of the grass mats in Hannover (Figure 3.20) by means of a fork lifter, the 80 grass sods were stored outside the Large Wave Flume (Figure 3.21) to allow for continued natural growth with natural light and natural weather conditions. The disadvantage of doing so was an increase of the moisture content of the soil due to possible precipitation. In order to avoid this, the grass sods were covered with plastic cover in case of rainfall or snowfall forecast.

The wooden frame and the underlying wooden beams were removed before installation of the grass sods on the dike model. Each grass sod was afterwards placed with the fork lifter on a wooden framework (Figure 3.22) for further handling. Two holes were drilled into the underlying wooden plate and transport with the crane runway, which is installed in the Large Wave Flume, was prepared (Figure 3.23).

Figure 3.20 Unloading of the grass sods at the Coastal research Centre in Hannover.

Figure 3.21 Temporary storage of the grass sods outside the Large Wave Flume.

Figure 3.22 Grass sod on wooden frame for further handling.

Figure 3.23 Entrance and crane runway of the Large Wave Flume.

In order to avoid longitudinal joints running all way up both slopes, it was decided to install the grass sods in displaced order. The grass sods were installed transverse to the flume and in row. One row of grass sods consisted of three grass sods with lengths of 0.9m, 2.35m and 1.45m. These three lengths covered the entire width of the flume (5m). The row positions of the grass sods with lengths of 0.9m and 1.45m were switched in every row. The 2.35m long grass sod always remained as central grass sod. By that, longitudinal joints running up both slopes were avoided (Figure 3.24).

In order to get grass sods of 0.9m and 1.45m length, a number of 2.35m long grass sods had to be cut. First the underlying wooden plate was cut using a circle saw then the grass sod was cut with a steel wire. For transportation of the grass sods from the entrance of the Large Wave Flume to the dike model, a steel beam and a wooden transport frame were used to hook the grass sod to the crane runway (Figure 3.25). The wooden transport frame was installed between the steel beam and grass sod to avoid the tilting of the grass sod during transport (Figure 3.26). The steel beam was tightened to the grass sod and wooden transport frame with ropes (Figure 3.27). Three different steel beams and two different wooden frames were used due to the different sizes of the grass sods. On each wooden plate two hooks were installed in order to pull the wooden plates underneath the grass sod after being placed on the dike slope.

Figure 3.24 Displaced order on the seaward dike slope.

Figure 3.25 Transport of grass sods by crane runway.

Figure 3.26 Wooden transport frame, steel hooks and two steel beams.

Figure 3.27 Tightening the grass sod to the transport frame and the steel beam with synthetic ropes.

At the dike model, the grass sod was placed on this installation position (Figure 3.28) and the wooden transport frame, steel beam and ropes were removed. After all three grass sods of one row were installed, the steel hooks (Figure 3.29), that were rigged before, were connected to a second set of synthetic ropes (blue ropes in Figure 3.30). A wooden beam (5m long) was then installed above the row of grass sods (Figure 3.31) by fixing it between the flume walls using wooden wedges. The function of the wooden beam was to provide a bearing in the later process of removing the wooden plates under the grass sods.

In order to remove the wooden plates, the crane runway of the Large Wave Flume was again used. The synthetic ropes were connected to one end of a steel cable (Figure 3.32) and the other end of the steel cable was hooked to the crane. The steel cable was led over a

deflexion pulley to avoid a lean traction as the crane hook just moves in vertical direction. The deflexion pulley was fixed to a strong beam, which was placed across the flume (Figure 3.33).

Figure 3.28 Installation of the third grass sod of a row.

Figure 3.29 Steel hook.

Figure 3.30 Installed grass sods including the underlying wooden plate and the steel hooks.

Figure 3.31 Wooden beam fixed between both flume walls.

Figure 3.32 Steel cable and connected synthetic ropes.

Figure 3.33 Crane hook, deflexion pulley and steel cable.

First the wooden plate under the 2.35m long grass sod was removed followed by the two smaller grass sods (Figure 3.34). After installation of the grass sods all gaps and joints

between the sods and the concrete flume walls were closed with clay. The clay being filled in the joints was compacted by hand.

The installation of the grass sods was started at the toe of the seaward slope and was continued up to the dike crest. Afterwards the grass sods on the landward slope were installed again starting at the toe. Finally, grass sods were installed at the dike crest and the grass cover was closed (Figure 3.35). After installation of the entire grass cover all gaps were again checked, especially the joints between the flume walls and the grass sods.

Figure 3.34 Pulling the underlying wooden plate.

Figure 3.35 Dike crest with grass cover.

In order to plane the grass surface and to strengthen the connection between the grass sods and the underlying clay layer, the grass sods were compacted by using a vibrating plate (Figure 3.36). After a couple trials on the seaward slope, local damage of the grass cover occurred (red circles in Figure 3.36 and Figure 3.37) and the compaction of the grass sods was stopped.

Figure 3.36 Compaction of grass layer on seaward slope.

Figure 3.37 Damaged grass surface due to compaction.

3.5 Artificial lightning and irrigation of the grass cover

Artificial lighting of the grass cover was needed as the light quantity inside the Large Wave Flume was not enough to support grass growth. In order to establish the best conditions for grass growth, special lamps were used for illumination. Each lamp had a power of 800W.

Figure 3.38 Illumination of the landward slope.

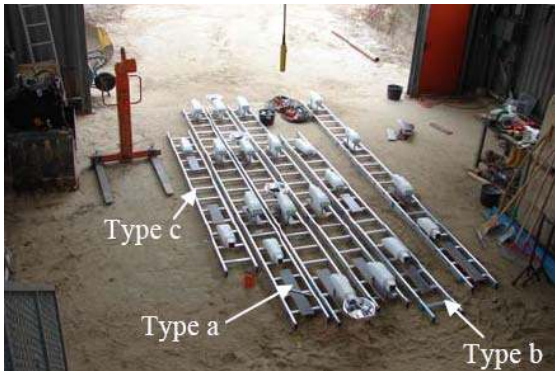

Figure 3.39 Six sets for artificial lightning of the grass cover.

Six illumination sets in three different sizes (Figure 3.39) were hung up 2.0m above the grass cover parallel to the dike surface (Figure 3.38 and Figure 3.40). The large illumination set consisted of four lamps (Figure 3.39, type a). The medium set comprised three lamps (Figure 3.39, type b) and the small set consisted of two lamps (Figure 3.39, type c). The lamps were rigged to aluminium ladders that were available in three different lengths. This construction was chosen in order to have a light construction that allowed to be carried by two persons.

The lamp sets were hung up above the dike surface with sisal ropes. The ropes were fixed to the railing at both sides of the flume. Since the sets had to be removed before the tests and installed again after the tests, flexible fasteners were used. The sets were moved by the crane runway and deposited on the flume gangways during testing. The installation and displacement of all six sets took about 30 minutes.

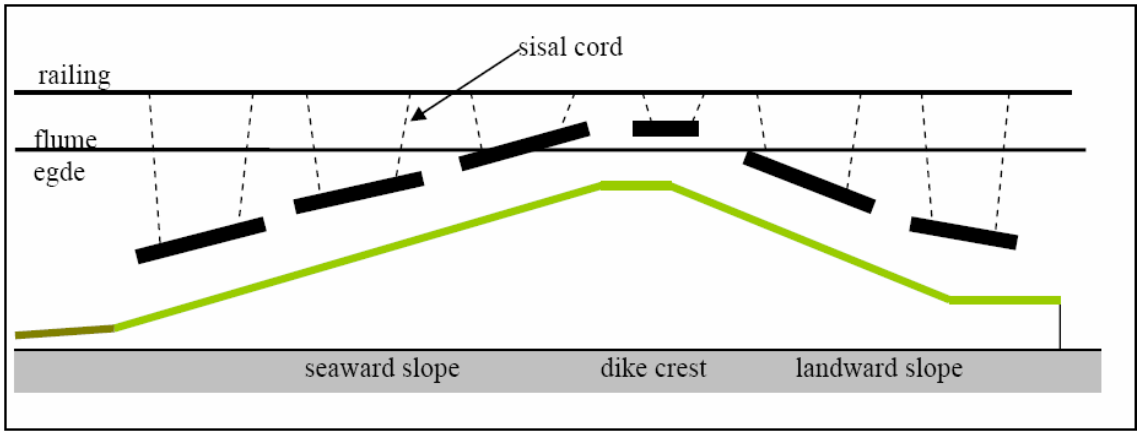

Figure 3.40 Cross view of the positioning of the artificial illumination sets.

The grass cover was illuminated during the recovery period, which was a 4-week long period between the end of construction and the start of the test programme. This period was chosen to allow the grass cover to recover after installation. During the recovery period the lamps

were switched on 24 hours long. During the test period, the grass cover was only illuminated between the test runs.

Figure 3.41 shows the positioning of the illumination sets. On the seaward slope three large sets (type a) were installed. The dike crest was party illuminated by the most upper set (type a) of the seaward slope and by a short set (type c). The toe of the landward slope was illuminated by a medium set (type b) and the lower part of the landward slope was illuminated by a large set (type a).

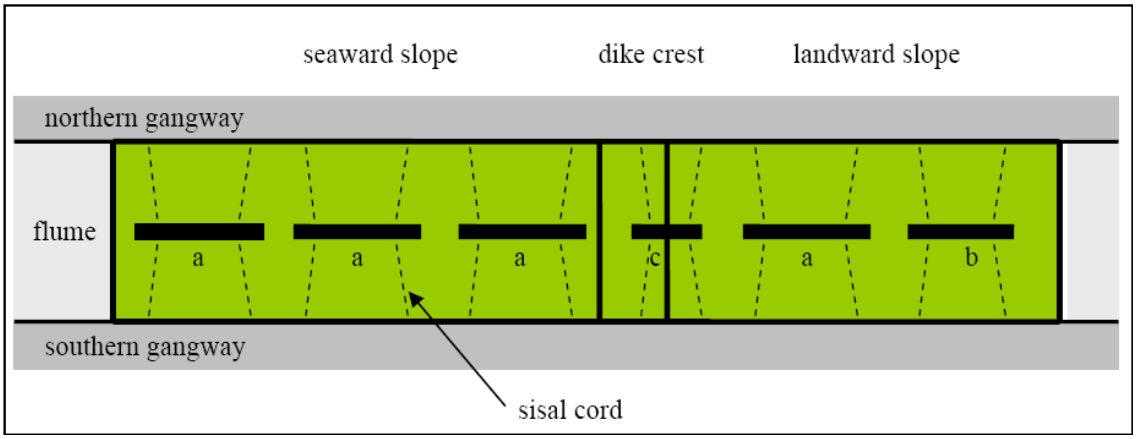

Figure 3.41 Plan view of the positioning of the artificial illumination sets.

Before beginning of the second test phase (se section 5), an overtopping container was installed above the landward slope. Installation of the overtopping container caused, however, that the position of the large lamp set (type a) and the medium lamp set (type b) had to be changed.

During the recovery period the grass cover was irrigated four times using a common irrigation system (Figure 3.43). Furthermore, the grass cover was mowed 3 times using a power mower since the slope of the landward side was too steep for a simple lawn mower (Figure 3.42). After mowing the stem length was between 4 and 5cm. The swath was removed to avoid mouldering of the grass.

Figure 3.42 Mowing the grass cover on the seaward slope.

Figure 3.43 Irrigation of landward slope.

3.6 Pumps

Two pumps, being available at the Large Wave Flume, were installed on the landward side of the dike model to empty the reservoir for overtopping water. The overtopping water was pumped back to the seaward side of the dike model. The pumps were connected to the internal pipe system of the Large Wave Flume by using steel pipes (Figure 58). The pump wells were protected with a fine wire mesh to avoid suction of broken grass leaves and swards. The wire mesh was fixed around the pumps by using small sand containers which were placed on the flume bottom (Figure 3.44, red circle). After each test run for wave overtopping the wire meshes were cleaned to avoid a decrease of the pumping capacity.

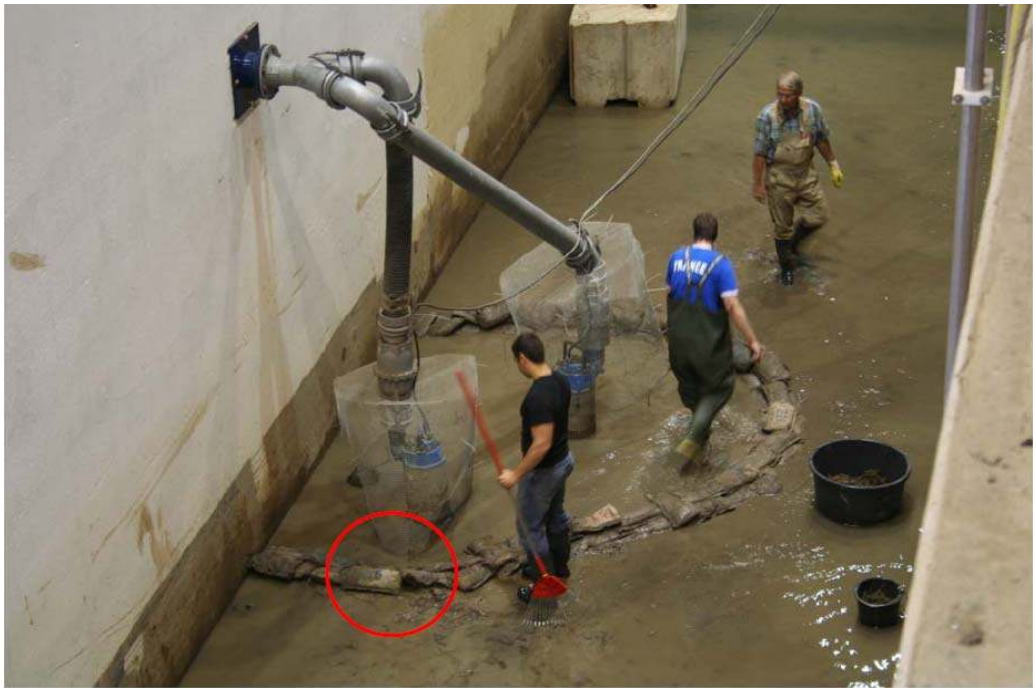

Figure 3.44 Two pumps on the landward side.

4. Measuring and observation techniques

The main objective of the test programme was to investigate the failure of the grass layer on the seaward and landward slope due to (i) wave impact, (ii) wave run-up and run-down flow and (iii) wave overtopping. For this purpose measuring and observation devices were installed on both dike slopes, such as:

- Wave gauges
- Pressure transducers
- Velocimeters (mini-propellers)
- Overtopping container
- Video and photo cameras

The used measuring and observation devices are described in the following. The description includes, besides technical data, also the type of installation and the positioning at the dike model.

4.1 Wave gauges

Three arrays including four wave gauges each were installed. The positions of the wave gauges are listed in Table 4.1 (see also Figure 4.1).

Table 4.1 Location of wave gauges.

Array	Wave gauge	Distance from the wave paddle
Array 1	1	50,1m
	2	52,2m
	3	55,9m
	4	61,3m
Array 2	5	79,05m
	6	81,15m
	7	84,85m
	8	90,25m
Array 3	9	116,0m
	10	118,0m
	11	120,0m
	12	122,0m

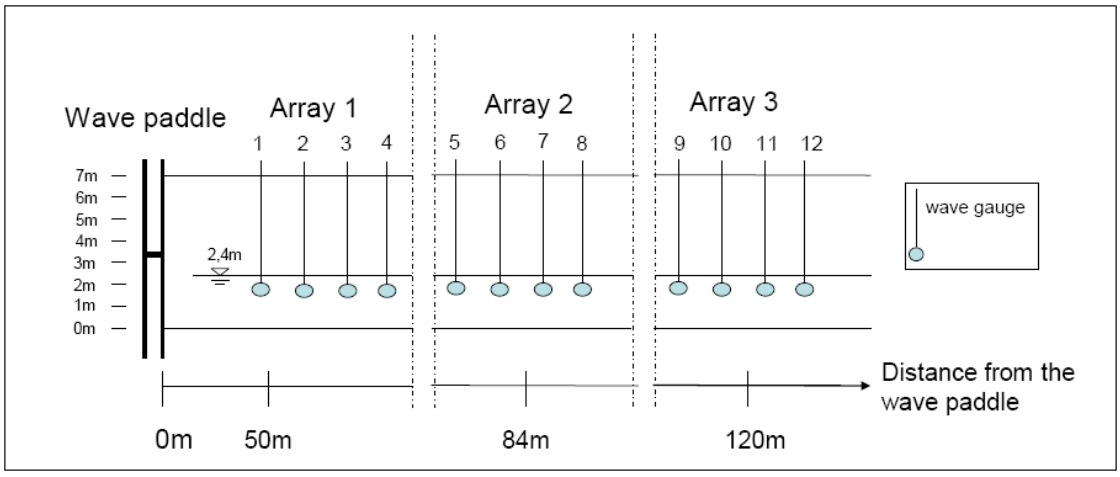

Figure 4.1 Position of wave gauges relative to the wave paddle in the flume

4.2 Pressure transducers

To measure the wave impacts on the seaward slope, five pressure transducers (PT) with a capacity of 5bar were installed on the seaward slope. The distance between two pressure transducers was approximately 1.25m corresponding to the width of the grass sod rows. The horizontal distance was 1.2m (Figure 4.2). This distance was chosen to avoid an installation of the transducers inside one grass sod, since it was expected that this would have a negative impact on the stability of the grass sod as the grass sod would had to be cut or a channel had to be dug through the sod. The distance of the pressure transducer from the flume wall was 1.2m.

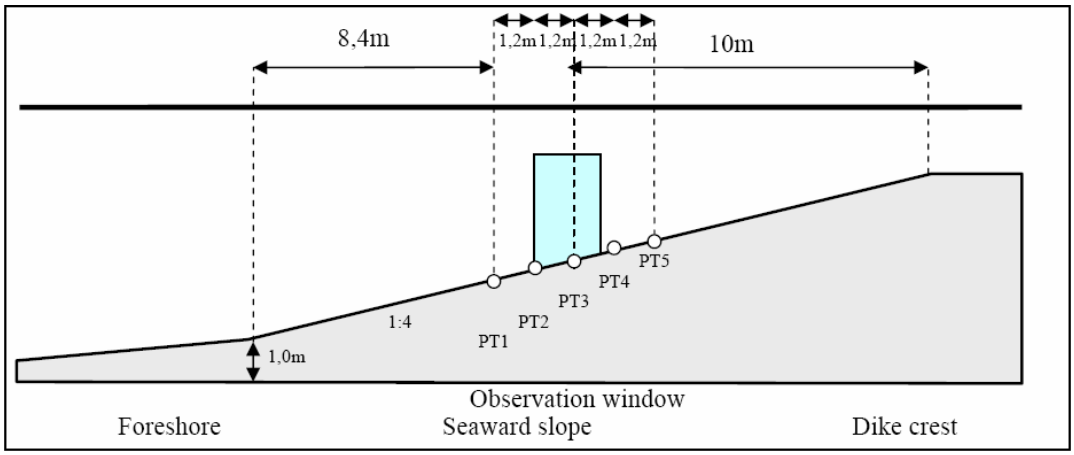

Figure 4.2 Location of pressure transducers (PT) on the seaward slope.

For installation of the pressure transducers five green plastic pipes were placed in a depth of 10cm in the clay layer before installation of the grass sods (Figure 4.3). A thin pull rope was installed in the cladding tubes (Figure 4.4) to pull the measuring cable that connects the pressure transducer to the receiver. Figure 4.5 and Figure 4.6 show the installed cladding tubes in the grass cover layer.

The pressure transducers were installed at the end of the recovery period of the grass cover. The plug connector of the transducer was pulled through the cladding tube together with a new pull rope, in the case that a pressure transducer got damaged and had to be changed

during testing. The transducer was mounted to a 1m long and 12mm thick reinforcing steel which was driven into the clay layer. The transducer was flushed with the topsoil surface and the hole and cladding tube were filled with clay to avoid intrusion of water (Figure 4.7 and Figure 4.8).

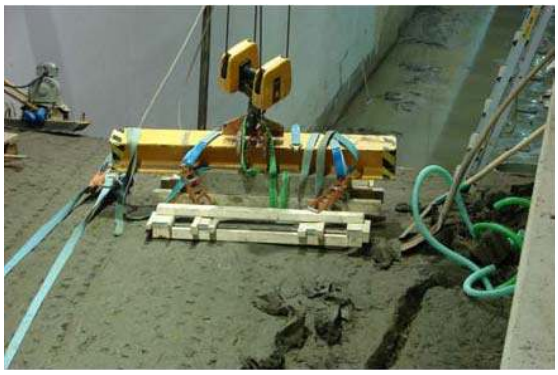

Figure 4.3 Channel for the cladding tubes.

Figure 4.4 Empty cladding tube including the pull rope inside.

Figure 4.5 Positioning of the empty cladding tubes.

Figure 4.6 Measuring cables and cladding tubes.

Figure 4.7 Installed pressure transducer.

Figure 4.8 Pressure transducer after a test run.

4.3 Velocimeters (Mini-propellers)

On the seaward slope five "Schiltknecht" mini propellers (head diameter of 22mm) (Figure 4.10) were installed to measure the velocity of run-up and run-down flow. The positioning and orientation of the propellers is shown in Figure 4.9 and Figure 4.12. The "Schiltknecht" mini propellers range from 0.02 to 5.0m/s. To avoid disturbances of the propeller by the grass cover or by grass swards, the propellers were installed at an adequate distance above the grass cover (Figure 4.11). Furthermore, the grass sward was cut in the areas around the propellers.

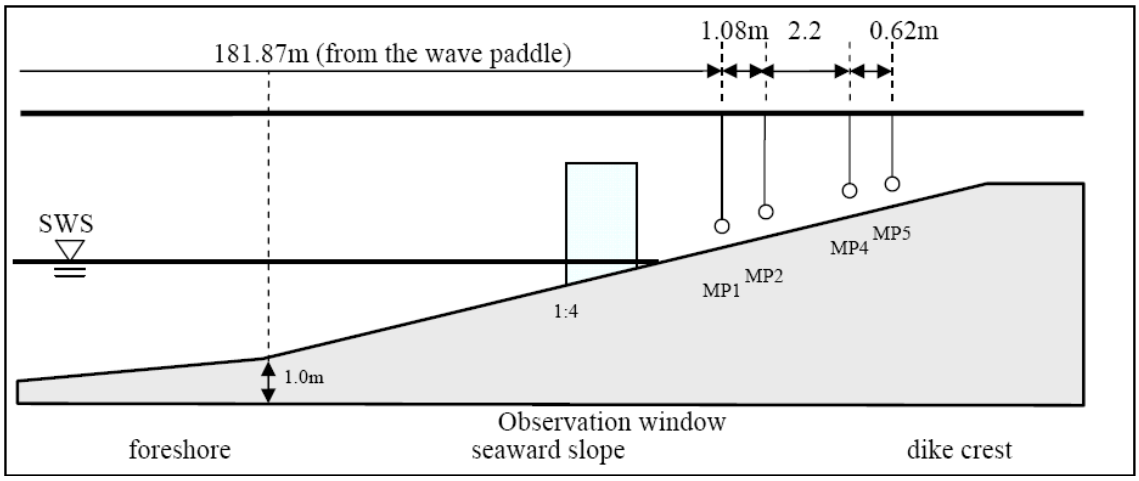

Figure 4.9 Locations of "Schiltknecht" mini propellers.

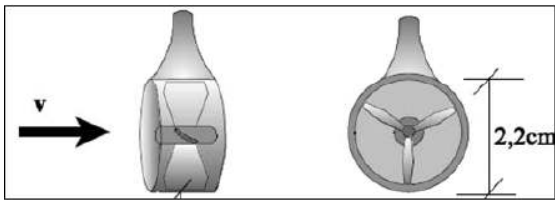

Figure 4.10 Schiltknecht" mini propeller.

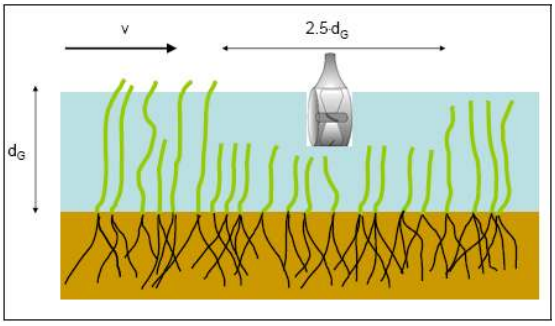

Figure 4.12 Orientation of mini propeller.

Figure 4.11 Installed "Schiltknecht" mini propeller.

4.4 Overtopping container

To measure the overtopping volume, an overtopping container was installed at the landward slope. The container was located 4.0m from the landward edge of the dike crest and consisted of a steel frame (Figure 4.13), a container, an inlet and a pump. The rigid steel frame was mounted at two steel beams above the landward dike slope. The steel beams

(Figure 4.13, left side) were placed across the flume and bolted to the gangway at both sides of the wave flume with built-in u-profiles. The installed steel frame and its position in the flume are shown in Figure 4.14.

The container was seated on three bearings. Two bearings were rigid and the third bearing consisted of a load cell. This transducer recorded the weight of the container while it was filled with overtopping water. The entrance of the inlet (Figure 4.15) was located at the landward edge of the dike crest. To avoid the inflowing water to overflow the container, a rebound wall was fixed to the container wall opposite to the end of the inlet (Figure 4.16).

Figure 4.13 Steel frame of the overtopping container.

Figure 4.14 Installed steel frame in the flume.

Due to the limited capacity of the overtopping container, the captured water had to be removed continuously to avoid an overflow of the container. The water was pumped over a hose (Figure 4.16) into the reservoir behind the dike model.

Figure 4.15 Inlet of overtopping container.

Figure 4.16 Overtopping container and hose system to empty the container.

4.5 Observation techniques

Video cameras

All tests were recorded by two digital video cameras. The two digital JVC cameras, including a hard disk of 60GB (GZ-HD3E), produced videos having a resolution of 1440x1080. The locations of the video cameras were changed depending on the test phases.

Phase 1 – Wave impact

During tests including wave impact (phase 1), the digital cameras were installed on the southern gangway of the flume (Figure 4.17), one camera pointing towards the seaward slope (Figure 4.18) and the other one pointing in the opposite direction (Figure 4.19).

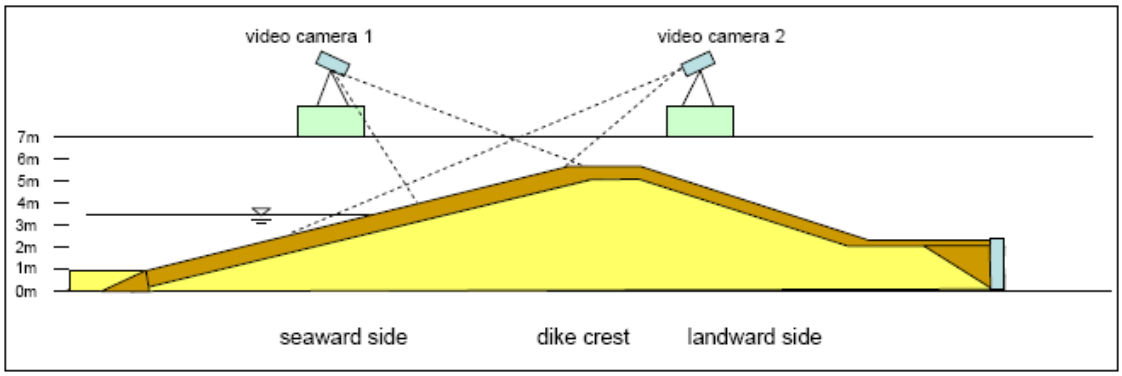

Figure 4.17 Camera locations during wave impact tests (phase 1).

Figure 4.18 View from camera 1.

Figure 4.19 View from camera 2.

Phase 2 – Wave overtopping

During tests comprising wave overtopping (phases 2), the digital video cameras were also installed on the southern gangway of the flume (Figure 4.20). One video camera was installed above the seaward slope pointed towards the dike crest (Figure 4.21). The second camera was installed at the landward side of the dike model pointing towards the landward slope (Figure 4.22).

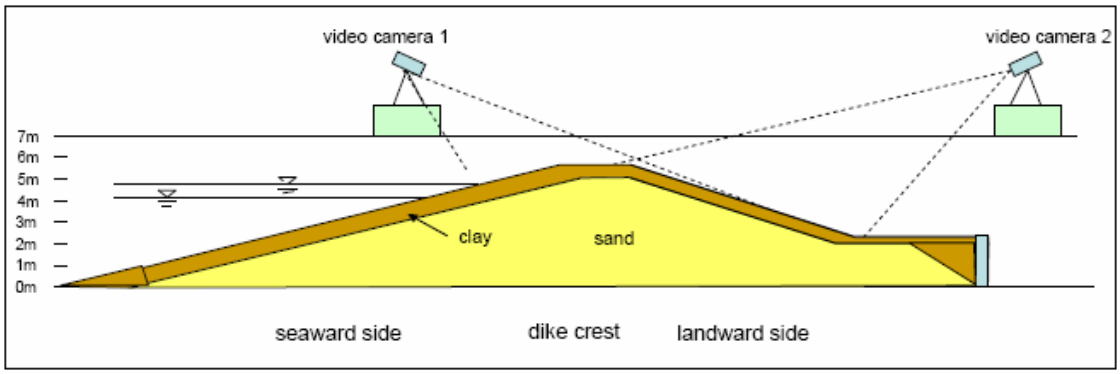

Figure 4.20 Camera locations during wave overtopping tests (phase 2).

Figure 4.21 View from camera 1.

Figure 4.22 View from camera 2.

Photo cameras

Grass sods, which were damaged during wave impact tests, were photographed after each test run. Degradation of a grass sod, being located at the northern flume wall in the third row (row C), is shown in Figure 5.24. The signboard in Figure 4.23 shows the hydrodynamic parameters of the test performed before the photo was taken. The first number in the first row defines the peak period T_p ('50' = 5.0sec.). The second number represents the significant wave height H_s ('08' = 80cm) and the last number stands for the water depth d ('37' = 3.7m). The abbreviations in the second and third row stand for 'SS' = seaward slope and 'C-L' is the identification code of the grass sod ('C' = row C; 'L' = left grass sod of the row form the middle). Identification of the rows starts with 'A' at the seaward toe in upward direction. The

last row at the landward side is marked with code ‘P’. The positions of the grass sods in one row are coded with ‘L’ = left grass sod, ‘M’ = middle grass sod, and ‘R’ = right grass sod. The positions of the grass sods are defined by standing in front of the dike model and looking at the seaward slope. In some cases, the middle grass sod was coded with ‘ML’, ‘MM’ and ‘MR’. ‘ML’ means left side of middle grass sod, ‘MM’ stands for the middle part of the middle grass sod, and ‘MR’ represents the right side of the middle grass sod.

The last row on the signboard informs about the date of the photo.

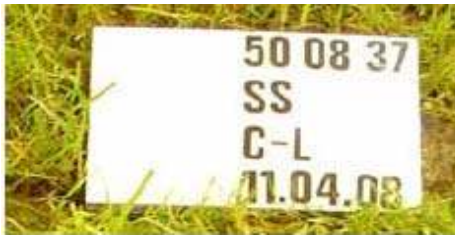

Figure 4.23 Signboard.

Figure 4.24 Degradation of grass sod L in row C after a series of wave impact tests.

Grid

After installation of the grass cover a grid was painted on the northern flume wall. The distance between the vertical lines was 1.0m, whereas the distance between the horizontal lines was 0.5m. The grid was painted following the entire dike surface (seaward slope, crest, landward slope) (Figure 4.21 and Figure 4.22).

5. Test programme

The test programme was divided into two phases. In the first phase the initiation of grass erosion on the seaward slope due to wave impact and wave run-up and run-down flow was studied. In the second phase the initiation of grass erosion on the landward slope due to wave overtopping was investigated.

In the following, a short overview of the hydraulic parameters of all performed tests is given. Afterwards both test phases are described including photos of the tests and example plots of the measured data.

5.1 Hydraulic parameters

The applied wave spectra based on a TMA spectrum. The water level in the flume was kept constant during test phase 1 and test phase 2. The effect of a tide could not be simulated in the flume.

The following tables list the hydraulic parameters of each test run, i.e. peak period T_P, significant wave height H_S and the water depth d. The parameters of the wave impact tests (phase 1) are listed in Table 5.1. Table 5.2 shows the hydraulic parameters of the wave overtopping tests (phase 2).

Table 5.1 Hydraulic parameter of wave impact tests (phase 1).

Impact	Impact	Impact	Impact	Impact
T_p = 4.0s	T_p = 5.0s	T_p = 5.0s	T_p = 5.0s	T_p = 6.0s
H_s = 0.5m	H_s = 0.7m	H_s = 0.8m	H_s = 0.9m	H_s = 0.5m
d = 3.7m	d = 3.7m	d = 3.7m	d = 3.7m	d = 3.7m

Table 5.2 Hydraulic parameter of wave overtopping tests (phase 2).

Overtopping	Overtopping	Overtopping	Overtopping
T_p = 5.0s	T_p = 5.5s	T_p = 6.0s	T_p = 6.5s
H_s = 1.0m	H_s = 0.75m	H_s = 0.85m	H_s = 0.9m
d = 4.7m	d = 5.0m	d = 5.0m	d = 5.0m

After each test the Large Wave Flume was drained for water, which lasted about 4 hours. The filling of the flume took about 5 hours. Consequently, testing was normally interrupted by one day with no tests.

5.2 Phase 1: Wave impact

The first test phase included the wave impact tests. After each test run damage of the grass cover was surveyed and documented by photos. In the case the grass cover was damaged, the grass sod concerned was removed and replaced by a new grass sod.

The wave run-up was recorded by video camera 1 (Figure 5.1). The shape of the breaking wave was recorded by camera 2 (Figure 5.2).

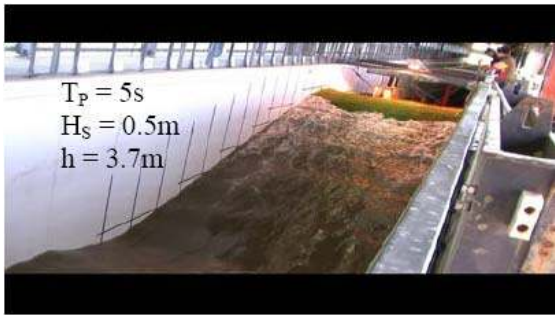

Figure 5.1 Wave run-up.

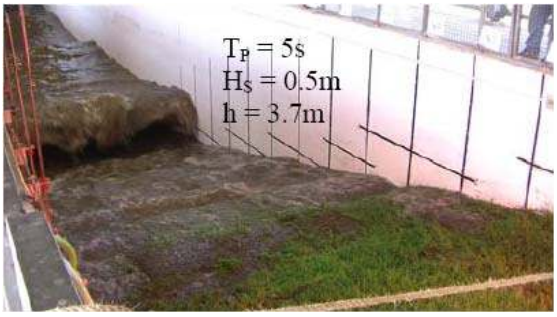

Figure 5.2 Wave breaking.

5.2.1 Example records of wave pressure

The main focus of test phase 1 was the effect of wave impacts on the grass cover and clay layer underneath. The wave pressure on the seaward slope due to wave breaking around the still water level was measured by five pressure transducers (see section 4.2, Figure 4.2). In addition, the waves on the seaward slope were measured by wave gauges. Wave run-up and the breaker type were recorded by video cameras (Figure 4.17 and Figure 4.18).

The following plots in Figure 5.3 to Figure 5.8 show the recorded wave height at wave gauge 12 (see Figure 4.1 and Table 4.1) and the recorded induced pressure impacts on the seaward slope in the area of wave breaking (Test 2204080).

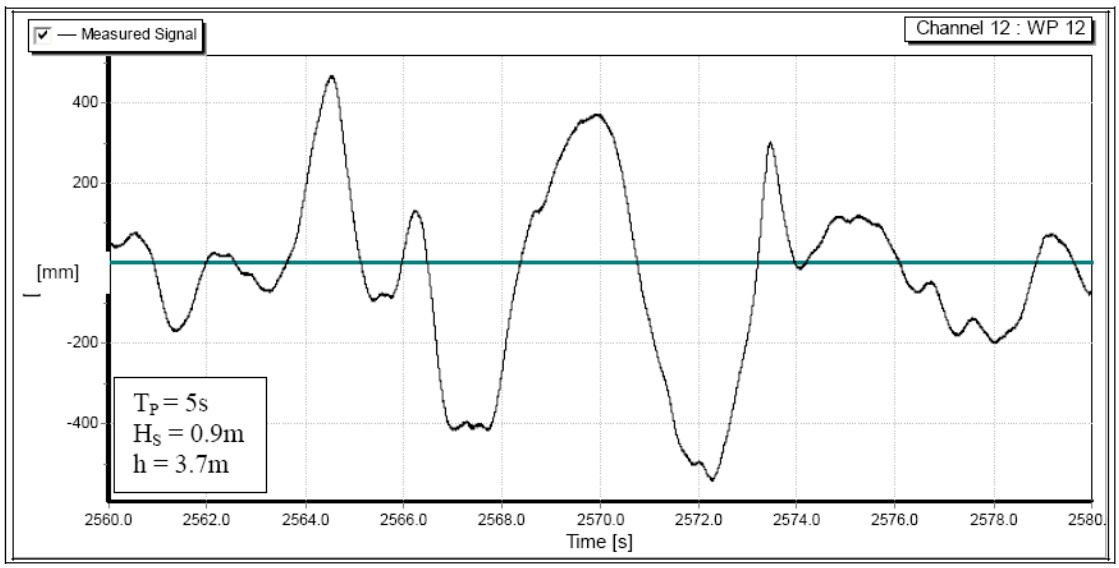

Figure 5.3 Recorded wave height at WG 12.

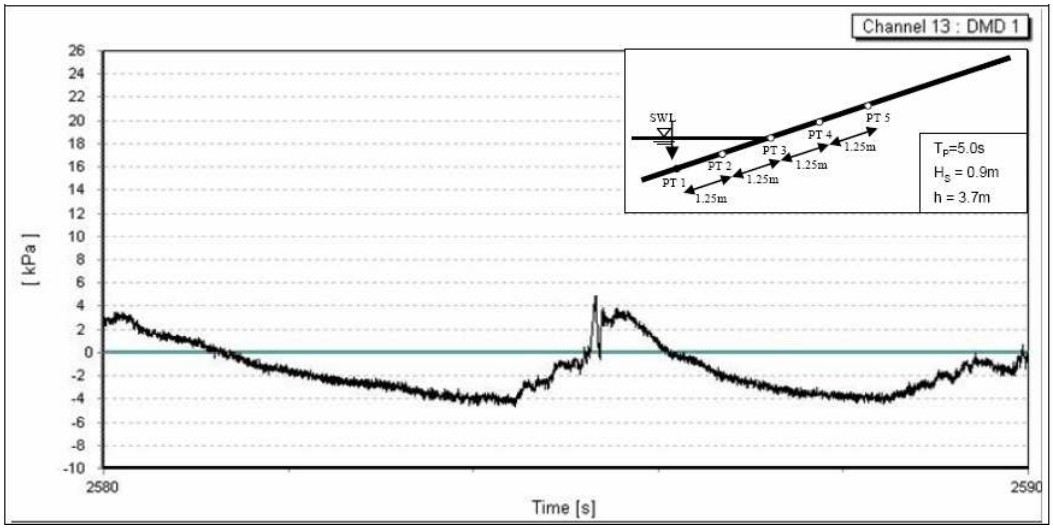

Figure 5.4 Recorded wave pressure on PT 1.

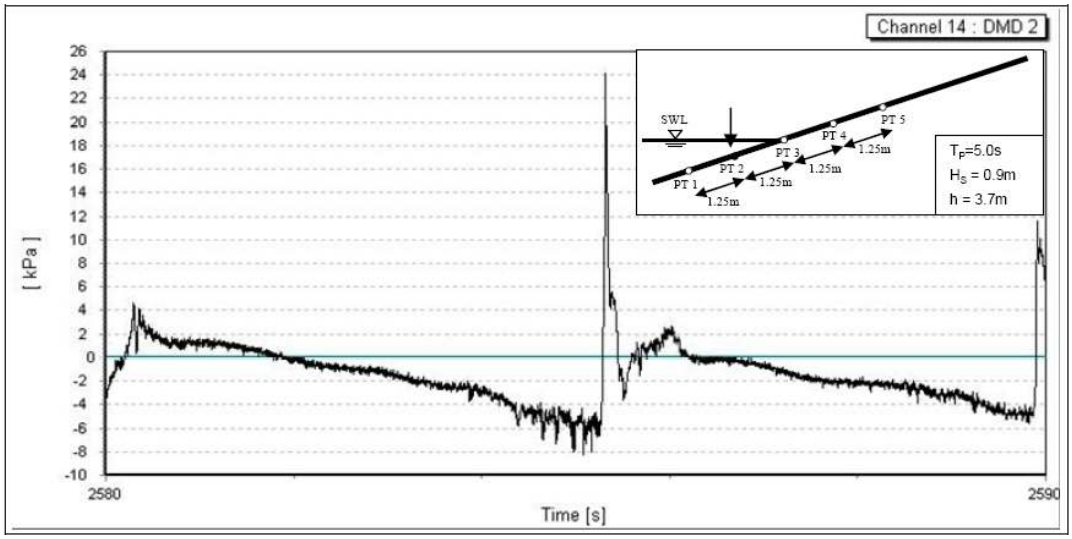

Figure 5.5 Recorded wave pressure on PT 2.

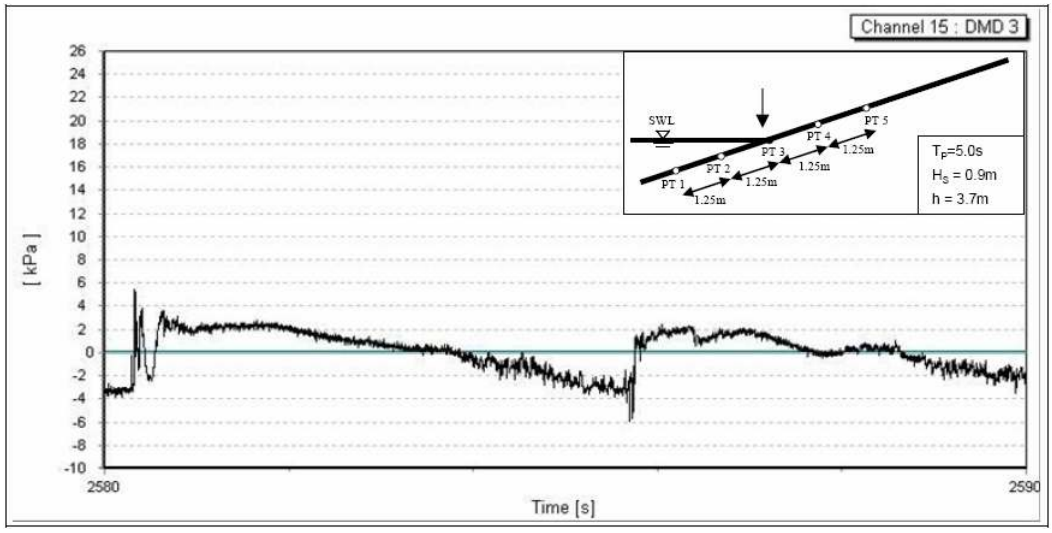

Figure 5.6 Recorded wave pressure on PT 3.

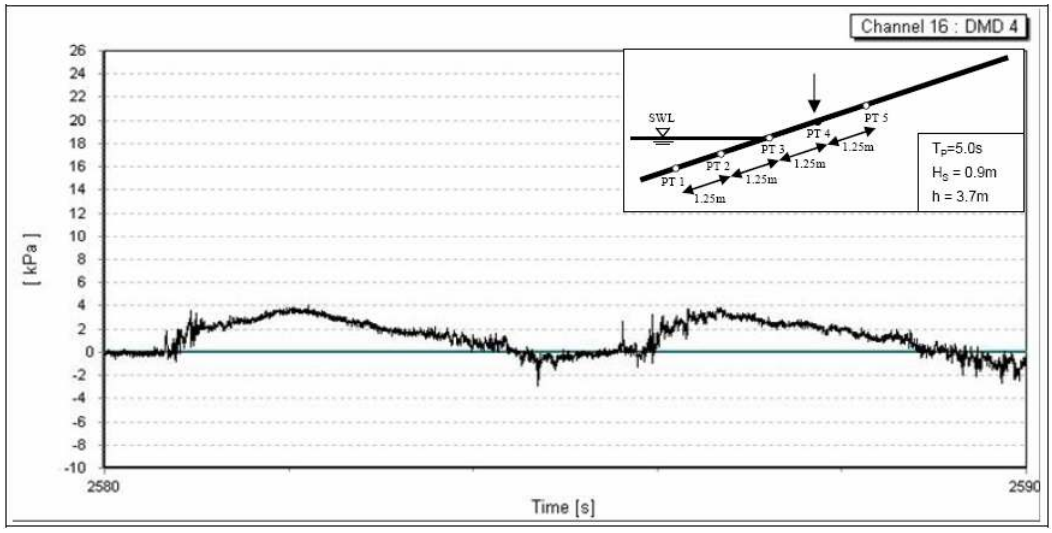

Figure 5.7 Recorded wave pressure on PT 4.

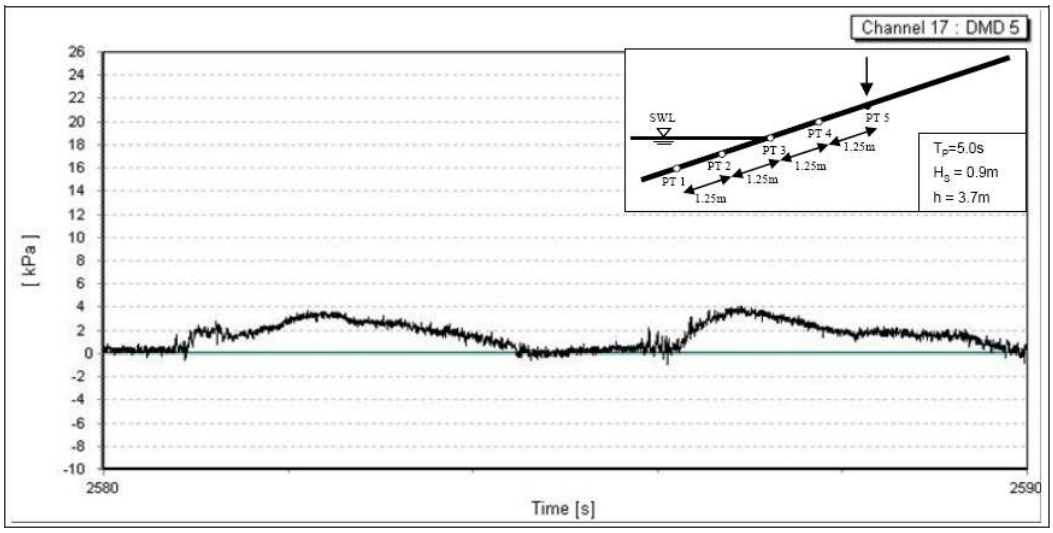

Figure 5.8 Recorded wave pressure on PT 5.

5.2.2 Example of recorded current metres

The following plots in Figure 96 to Figure 99 show the recorded run-up velocities on the seaward slope in the area of wave breaking (Test 2204080) for the hydraulic parameters of T_P = 5s, H_S = 0.9m and h = 3.7m.

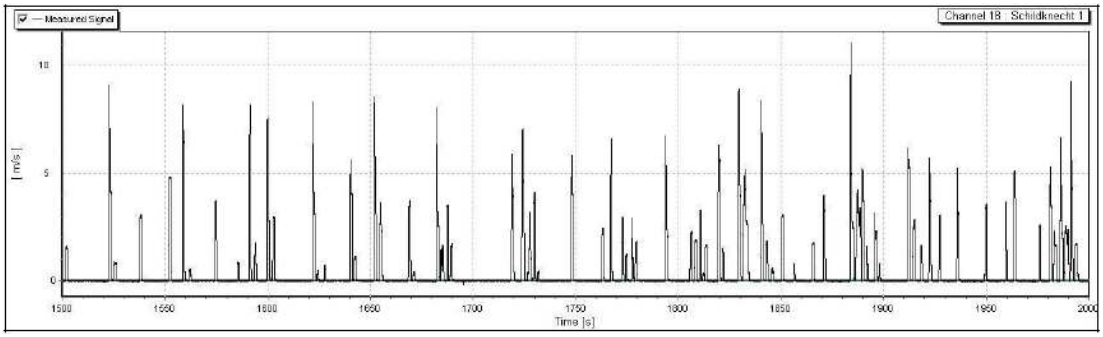

Figure 5.9 Recorded velocity at Schiltknecht propeller MP1.

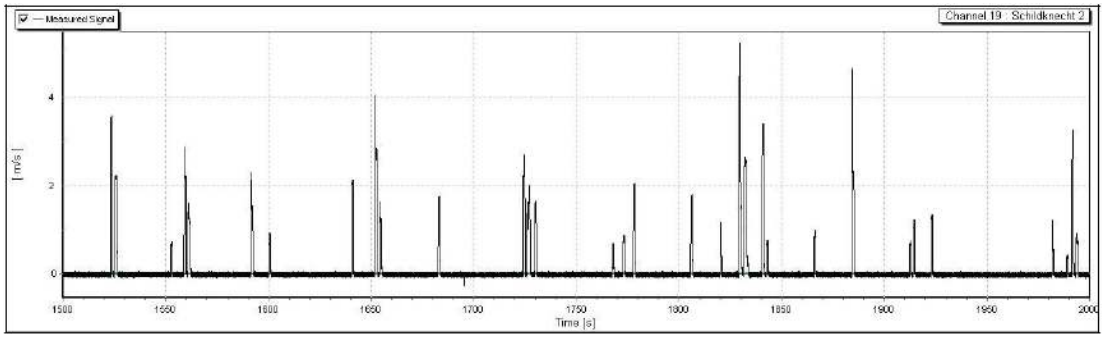

Figure 5.10 Recorded velocity at Schildknecht propeller MP2.

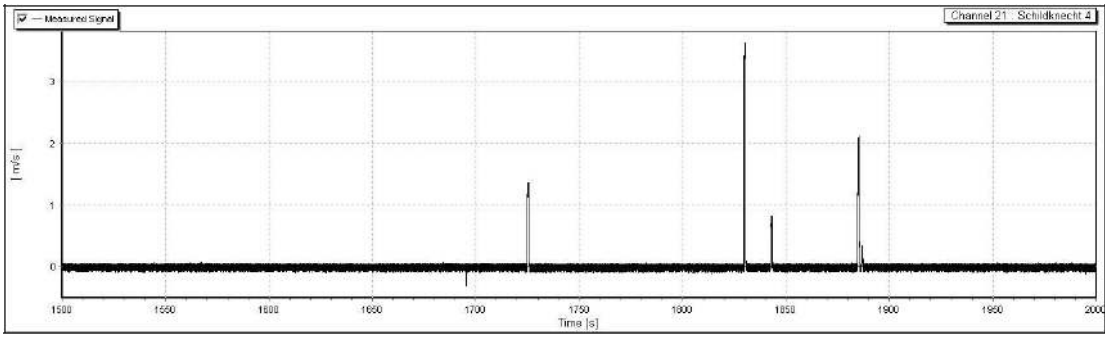

Figure 5.11 Recorded velocity at Schildknecht propeller MP4.

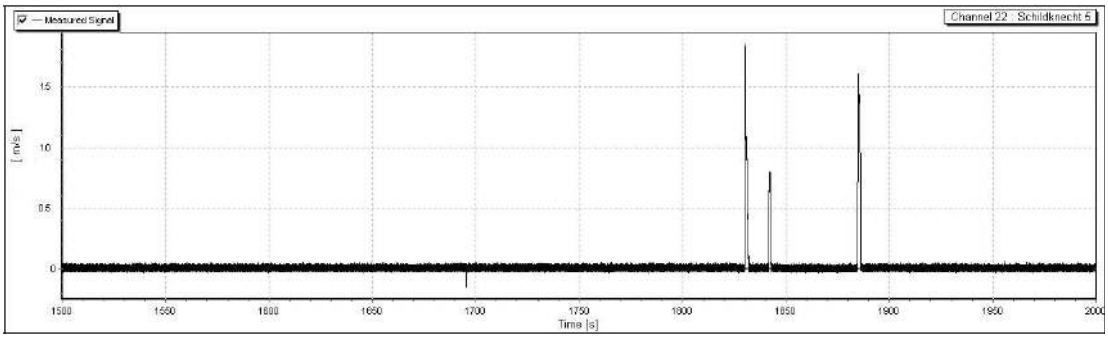

Figure 5.12 Recorded velocity at Schildknecht propeller MP5.

5.2.3 Wave run-up

The wave run-up heights are analysed based on the recorded videos.

Figure 5.13 Wave run-up height of 5.65m.

5.2.4 Damage of the grass cover due to wave impact

The grass cover was surveyed for damage after each test run with the objective to describe

- the instantaneous damage caused by single breaking wave impact events and
- the damage over the entire duration of the test.

Damage by single impact

The first damage of the grass cover occurred at the observation window in the flume wall during the tests on April 11th, 2008. The wave parameters were T_p = 5.0s, H_S = 0.9m. The water depth was about 3.7m. The damage was caused by a single impact. As shown in Figure 5.15, only a part of the 90cm wide grass sod was damaged. The original stage of the grass sod is shown in Figure 5.14. The dimensions of the damaged area are illustrated in Figure 5.16. The marked area A in Figure 5.16 shows, however, an area that was directly located at the observation window and not eroded. After investigation of the soil surface of the damaged part, it was noticed that the visible clay was not part of the clay layer, rather the clay of the grass cover as the hole was just 10cm deep (Figure 5.17).

Figure 5.14 Undamaged grass sod in front of the observation window (before breaking wave impact).

Figure 5.15 First damage on the observation window (after impact).

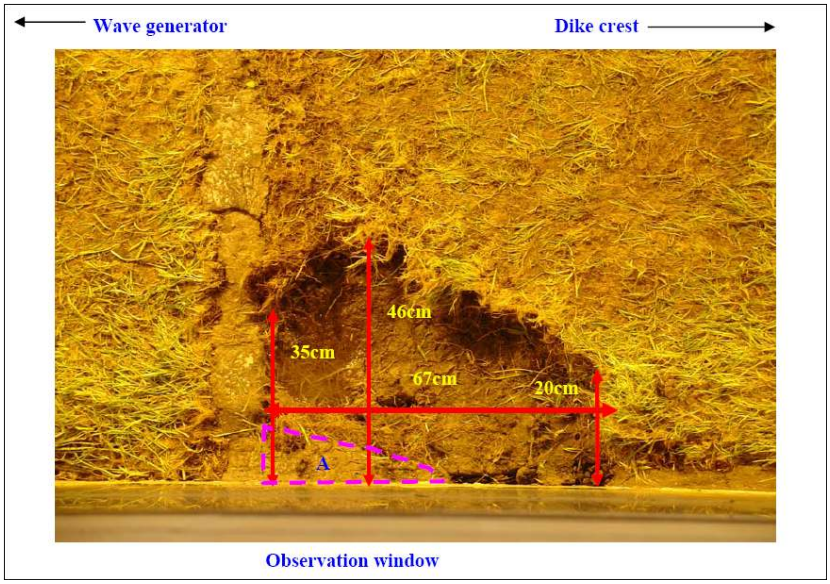

Figure 5.16 Dimensions of hole in the grass cover (max. scour depth ~10cm).

In order to repair the grass cover, the remaining grass sod (area A, Figure 5.16) and the underlying clay were removed. Moreover, the hole to be repaired was enlarged wherewith the new grass sod piece for repair had to size 53cm in width and 70cm in length (Figure 5.18 and Figure 5.19). The repaired grass sod can be seen in Figure 5.20.

Figure 5.17 Depth of hole.

Figure 5.18 Width of the prepared hole.

Figure 5.19 Length of the prepared hole.

Figure 5.20 Repaired grass sod.

Damages over entire test duration

During the entire test duration, different kinds of damage or stages of damage were observed. For example, round balls of different sizes were observed on the dike surface (Figure 5.21) and within the topsoil. It is however important to notice that the development of these balls was not the result of lose clay lumps being moved up and down the slope. The balls were also observed in the soil with a dense root network (Figure 5.22).

In some cases the clay material, which was used to close the joints between the grass sods, was removed and had to be replaced regularly. Moreover, small holes (Figure 5.23) were registered after the tests.

The degradation of the grass layer in the surf zone caused by the long testing period (phase 1 and phase 2) is shown in Figure 5.24. The grass cover (swords and leafs) in the lower part of the seaward slope remained longer green and alive than the grass within the breaker zone.

The grass cover that was permanently inundated was much less degraded than the grass cover in the breaker zone. After three days without testing, new small grass leafs were seen.

Figure 5.21 Formation of clay balls lying on the slope surface.

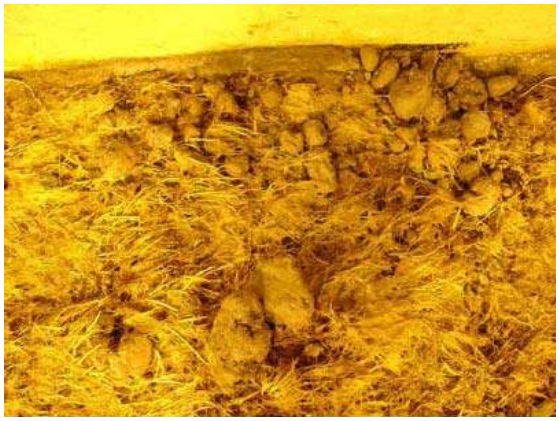

Figure 5.22 Formation of clay balls located in the grass sod.

Figure 5.23 Open joint between two grass sods.

Figure 5.24 Degradation of the grass cover in the breaker zone.

5.3 Phase 2: Wave overtopping

The objective of the wave overtopping tests was to investigate the effect of overtopping discharge on the grass cover and clay layer at the landward slope. The installed overtopping container (see section 4.4, Figure 5.25) was used to collect a certain part of the overtopping water. The load cell of the overtopping container recorded continuously the changing weight of the container due to the inflow of overtopping water through the inlet as well as due to the lowering of the water level in the container by pumping out the water. The overtopping processes on the landward slope and on the dike crest were recorded by video camera 1 (Figure 4.21) and video camera 2 (Figure 4.22).

Figure 5.25 View from the dike crest.

Figure 5.26 View from the area behind the dike model.

5.3.1 Example of wave overtopping records

The overtopping discharge was continuously measured over the entire test duration. Both individual and average overtopping discharge and their influence on the grass sods are analysed.

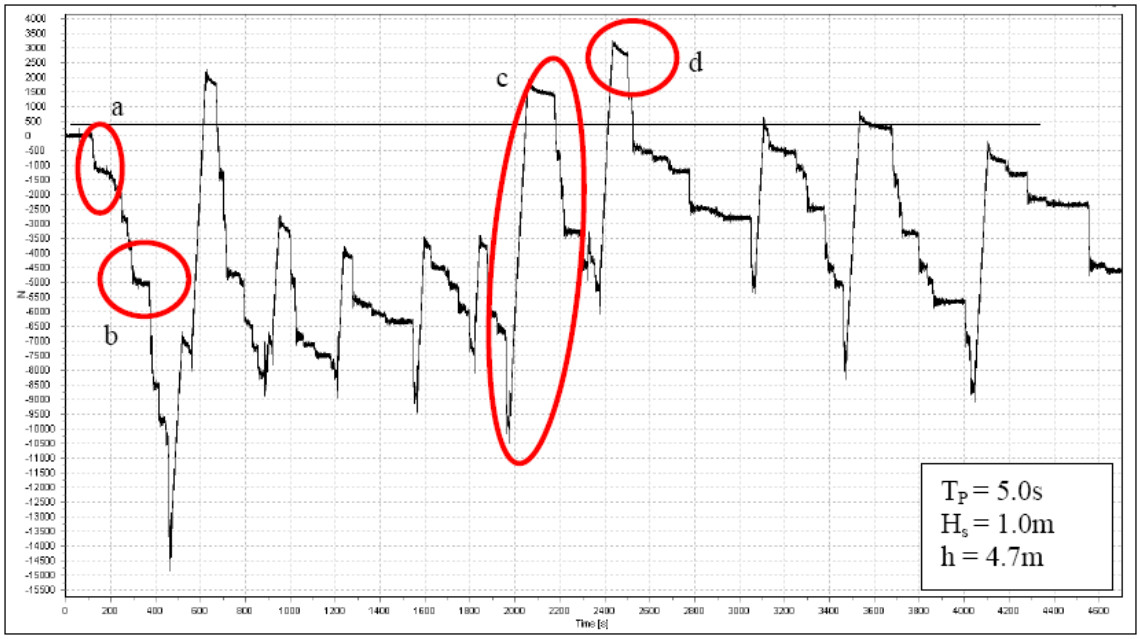

Figure 5.27 Record of the changing water volume in the overtopping container (Test 28040802).

Different distinctive points can be seen in Figure 5.27. In Point ‘a’ water flows into the container and its weight increases. In point ‘b’ a constant water level in the overtopping container can be noticed. When the maximum possible water level was reached in the container, the water was pumped out and the pressure decreased. This effect can be seen by the vertical line in point ‘c’. At the end of pumping out the water, the pressure increased again immediately (point ‘d’). This effect was caused by water which was still in the hose and flowing back into the container after the pumps were switched off.

Besides recording the load of the container, the start time and end time of pumping water out of the overtopping container, was written down. The start time and end time of pumping actions according to the record in Figure 5.27, are given in Table 5.3. In the case water had run-over the container, a remark was made in the table.

Table 5.3 Beginning and ending of pumping time (overtopping test 280408).

	Start	End	Remarks
1.	12:23:07	12:24:04	
2.	12:24:45	12:25:52	
3.	12:30:17	12:30:27	
4.	12:30:42	12:31:15	
5.	12:35:32	12:36:02	
6.	12:41:27	12:42:00	
7.	12:45:40	12:46:07	
8.	12:48:17	12:49:43	
9.	12:54:05	12:54:12	
10.	12:55:00	12:55:58	
11.	13:06:32	13:07:10	
12.	13:13:17	13:14:17	
13.	13:22:49	13:23:48	

5.3.2 Damage of clay and grass cover by wave overtopping

During the wave overtopping tests, parts of the seaward grass cover were damaged. Due to the increased water level, the breaker zone moved upwards whereby the damaged grass sods were found in row K (Figure 5.28). Furthermore, damaged joints between grass sods on the seaward slope were registered (Figure 5.29). Severe damage on the landward grass cover due to wave overtopping was not observed.

Figure 5.28 Damaged grass cover on the seaward slope during wave overtopping tests.

Figure 5.29 Damaged joint on the seaward slope during wave overtopping tests.

6. Concluding remarks and outlook

Large scale model tests have been performed to investigate in detail the failure of grass cover layers due to (i) wave impact, (ii) wave run-up and run-down flow and (iii) wave overtopping. Hence, the EroGRASS project dealt with the investigation of grass cover failure anywhere along the dike model profile, as wave impact as well as wave run-up and run-down flow may induce grass cover failure on the seaward slope and wave overtopping may cause grass cover failure on the dike crest and shoreward slope.

Valuable measurements and observations have been obtained in breaking wave impact and other processes such as wave up rush and down rush together with subsequent damage of the grass cover layer at the seaward slope. Furthermore, the loading of the grass cover on the shoreward slope was investigated.

6.1 Lessons learned

During the entire project a number of lessons were learned. These experiences are described in the following. The lessons learned during model set-up and model construction are described first, followed by the experiences gained during both test phases.

- The surface of the seaward and shoreward slope has to be improved by making them more even. This can be achieved if the grass sods have the same thickness. However, it is difficult to go for a constant thickness of each grass sod as the grass layer on a 'real' sea dike is a natural product. The method of excavating the grass sods at the Ribe dike showed that cutting the grass sods in horizontal direction is difficult but not impractical. Weather conditions during excavation of the grass sods were very poor. Less precipitation the days before excavation and a more advanced method to control the cutting depth will result in a more constant thickness of the grass sods.
- The approach used for installation of the grass sods has to be improved in the future. The method used implied that every grass sod had to be handled very carefully to avoid additional cracks and fissures. This again was very time-consuming and asked for much strenuous manual work. Tools, such as hydraulic shields, should be developed to reduce the amount of manual work. The disposability of only one crane in the Large Wave Flume turned out to be also time-consuming as the one crane was used for many operations which again resulted in a number of re-settings of the crane.
- Due to the natural structure of the grass sods, the surface of the installed grass cover was uneven. On the seaward side a couple of buckles were observed after installation of the grass cover layer. These buckles justified the attempt of using a compactor to regulate the surface and to improve the contact between the grass sods and the clay layer. However, the application of the compactor was difficult on the seaward slope and implicated local damage of the grass cover. The soil within the topsoil started to liquefy and moved up towards the surface. The grass swards were partly or completely covered by the soil.
- A further problem caused by the uneven seaward slope surface was the influence of the grass sod edges on the stability of the grass sod itself. In some cases, a small step between the lower and the upper grass sod was noticed, which were loaded by wave run-up.
- The lightening, mowing and irrigation of the grass layer was important and enabled the grass layer to grow satisfactorily.

During both phases of testing the following observations and experiences were made:

- After the first tests (phase 1) earth worms became active and aerated the topsoil and weakened the upper soil layer of the grass cover. Many small mounds of about 5mm in height were observed.
- The seaward slope of the dike model was selected to 1:4 in order to investigate wave impact on the grass layer. At this slope the run-down water was not able to act as a natural damper for the next wave impact. Therefore the boundary conditions for wave impact tests caused wave impact on the seaward dike slope without the advantage of natural damping by the run-down water of the foregoing wave. This again resulted in a faster degradation of the grass cover during testing. During the second test phase (wave overtopping), the seaward grass cover was already in a decayed condition that implied constant inspection of the entire seaward grass cover layer to avoid an overall failure of it. This development of the seaward grass cover could have been avoided if the seaward slope would have been 1:6. Furthermore, a simultaneous testing of the different wave loads on both dike slopes would have resulted in a more contemporaneous degradation of both grass covers on the seaward and landward slope.
- The horizontal dike toe on the landward side prevented a complete run-off of the overtopping water. Residual overtopping water remained in this area after each test run. Mouldering of the grass cover was not observed, but the quality of the grass in this area was less compared to other areas on the landward slope.
- No border effects or negative influence of the flume wall on the test runs was observed. Inspection of each grass sod and each joint after every test run was necessary and appropriate. Damage of grass sods and joints were, through this, found immediately.
- The pumping capacity to empty the overtopping container was not large enough. A maximum overtopping rate was limited to about 30l/(s m). Overtopping discharges larger than 30l/(s m) could not be measured without introducing measurement uncertainties as overtopping water swashed out of the container.
- The inlets of the pumps in the reservoir behind the dike model were very easily blocked. The blockage of the inlets decreased the pumping capacity which caused a rapid increase of the water level in the ‘hinterland’ and a decrease of the water level on the seaside by 10-20cm as the overtopping water was pumped back in front of the dike model. A simultaneous adjustment of the water level in front of the dike model through the flume inlet is not possible. Re-pumping of the overtopping water has therefore to be improved.

6.2 Outlook

The analysis of the obtained data, which has started, will focus on the following aspects:

- Analysis of the hydrodynamic processes associated with failure at the seaward dike slope and their implication for erosion. This includes data and observations concerning wave run-up and run-down velocities, layer thickness and the implication on erosion and other failure modes. Furthermore, the wave impact pressure caused by surging breakers will be analysed, which contains the effect of damping of wave impact due to a water layer of the preceding wave run-up, the analysis of the impact load time history as well as statistic analysis of impact pressure and force.

- Investigation of the hydrodynamic processes associated with grass cover failure and the implication of erosion at the dike crest and on the shoreward slope in relation to mean wave overtopping rates.

The analysis of the test data and the results will be published in a second project report at a later date.

Acknowledgement

The funding of the EroGRASS project comprising the investigations grass cover failure due to wave impact and wave run-up and run-down flows on a seaward dike slope as well as wave overtopping on the landward slope is gratefully acknowledged. The contributions of the GWK team, especially by Mr. Peter Geisenhainer and Mr. Uwe Sparboom, have been of enormous help and are therefore gratefully acknowledged in particular.

References

EAK (2002): Empfehlungen für Küstenschutzwerke. Die Küste, archiv für Forschung und Technik an der Nord- und Ostsee, Heft 65, Boyens & Co., Heide i. Holst.; Germany, 589 pages.

Möller, J.; Weißmann, R.; Schüttrumpf, H.; Kudella, M.; Oumeraci, H.; Richwein, W.; Grüne, J. (2005): Interaction of wave overtopping and clay properties for sea dikes. Proceedings 28th ICCE, Vol. 2, Cardiff, U.K., pp. 2105-2127.

Richwien, W.; Weißmann, R. (2001): Belastung der Binnenböschung von Seedeichen durch Wellenüberlauf. Abschlußbericht. Institut für Grundbau und Bodenmechanik, Universität und Gesamthochschule Essen, Teil III, Essen, Germany, pp. 40. (In Germany).

Smith, G.M.; Seijffert, J.W.W.; Van der Meer, J.W. (1994): Erosion and overtopping of a grass dike. Large scale model tests. Proceedings 24th International Conference on Coastal Engineering (ICCE), ASCE, Volume 3, Kobe, Japan, pp. 2639-2652.

Simon and Collison (2001): Quantifying root reinforcement of streambanks for some common riparian species: Are willows as good as it gets? ASCE, Wetlands Engineering and River Restoration Conference 2001, Reno, Nevada, USA.

Sprangers, J.T.C.M. (1999): Vegetation dynamics and erosion resistance of sea dyke grassland. Ph.D.-Thesis, Wageningen Agricultural University, Wageningen.

Stanczek, G. (2008): Breaching of sea dikes initiated from the seaside by breaking wave impacts. Ph.D. thesis, Dissertation, Civil Engineering Faculty, Leichtweiß-Institut für Wasserbau, Technical University Braunschweig, University Florence, Braunschweig, Florence.

TAW (1996): Technical Report – Clay for dikes. Technical Advisory Committee for Flood Defence, Delft.

TAW (1997): Technical Report – Erosion resistance of grassland as dike covering. Technical Advisory Committee for Flood Defence, Delft.

TAW (1999): Grass cover as dike revetment. Technische Adviescommissie voor de Waterkeringen (TAW), Delft, The Netherlands, 17p.

Temple, D.M.; Hanson, G.J. (1994): Headcut development in vegetated earth spillways. Applied Engineering in Agriculture, 10, pp. 677-682.

Temple, D.M.; Robinson, K.M.; Akring, R.M.; Davis, A.G. (1987): Stability design of grass-lined open channels. USDA Agricultural Handbook, No. 667.

Young, M. (2005): Wave overtopping and grass cover layer failure on the inner slope of dikes. MSc Thesis, UNESCO-IHE, Institute for Water Education, Delft, the Netherlands.

Young, M.; Hassan, R. (2006): Grass Cover Layer Failure on the Inner Slope of Dikes. 30th International Coastal Engineering Conference, San Diego, USA.

List of figures

List of tables

Appendix A: Preliminary Data Analysis Report

A1 Data analysis

Introduction

A brief overview of the collected data from EroGRASS project and some basic results from the preliminary data analysis are given in this note.

First, a description of concepts for data analysis is described in this section. Then, the methodology used for the preliminary analyse of incident wave parameters, mean wave overtopping discharge are described in following sections. The preliminary results of the data analysis and the discussion of the results are given in section 2. Appendix A: Preliminary Data Analysis Report

During the performed model tests following data were collected,

- wave conditions in front of the structure
- wave overtopping volume per wave
- wave overtopping flow velocity at seaward slope
- video records of wave impact on the seaward side and wave overtopping
- pressure measurements on the seaward slope of the dike

Detail description of the applied measuring equipments and their positions are given in Geisenhainer and Oumeraci (2008).

Data analysis tools

L~Davis, data analysis and visualisation software developed by LWI was the main tool for preliminary data analysis. L~Davis can perform reflection analysis, setting time frames, statistical analysis of generated waves in both time and frequency domain, signal filtering, Event analysis etc. Most of the tests were recorded with 500Hz frequency. Therefore, before analysing the data, correct data step should be set. For an example, the data step for the wave gauge data was selected as 10. Then, the frequency of the wave data set, which is used for the analysis, is 50Hz. Depending on the requirement and the expected accuracy, the data step for the all the channels should be carefully selected and set at the beginning of analysis.

A brief description of L~Davis is given on the website of Leichtweiß-Institute (LWI, http://www.lwi.tu-bs.de/hyku/english/en_Ldavis-index.html). Furthermore, the latest versions of L~Davis includes help files and has also the ability to upgrade to the latest version via internet.

Overview of Data

An overview of the available data is given in Table1.1. Each measuring device was calibrated before the tests. However the data of first 3 tests do not have calibration factors due to a problem during the data acquisition. Therefore, the calibration factors found on 2008.04.16 were used for the data analysis of the test conducted on 2008.04.08, 2008.04.10 and 2008.04.11. Since the test configurations were similar and the water from the same source was used, it was assumed, that the calibration factors were remained unchanged during this period. Results from the calibration test conducted afterwards justify the above assumption.

Furthermore, the “GTX” files (see Figure A1.1) of the data set from the test phase 1, are missing the locations of measuring instruments from Channel number 18 to channel number 27. Before start the analysis, positions of the measuring devices should be corrected in all the “GTX” files. L~Davis software facilitates this operation.

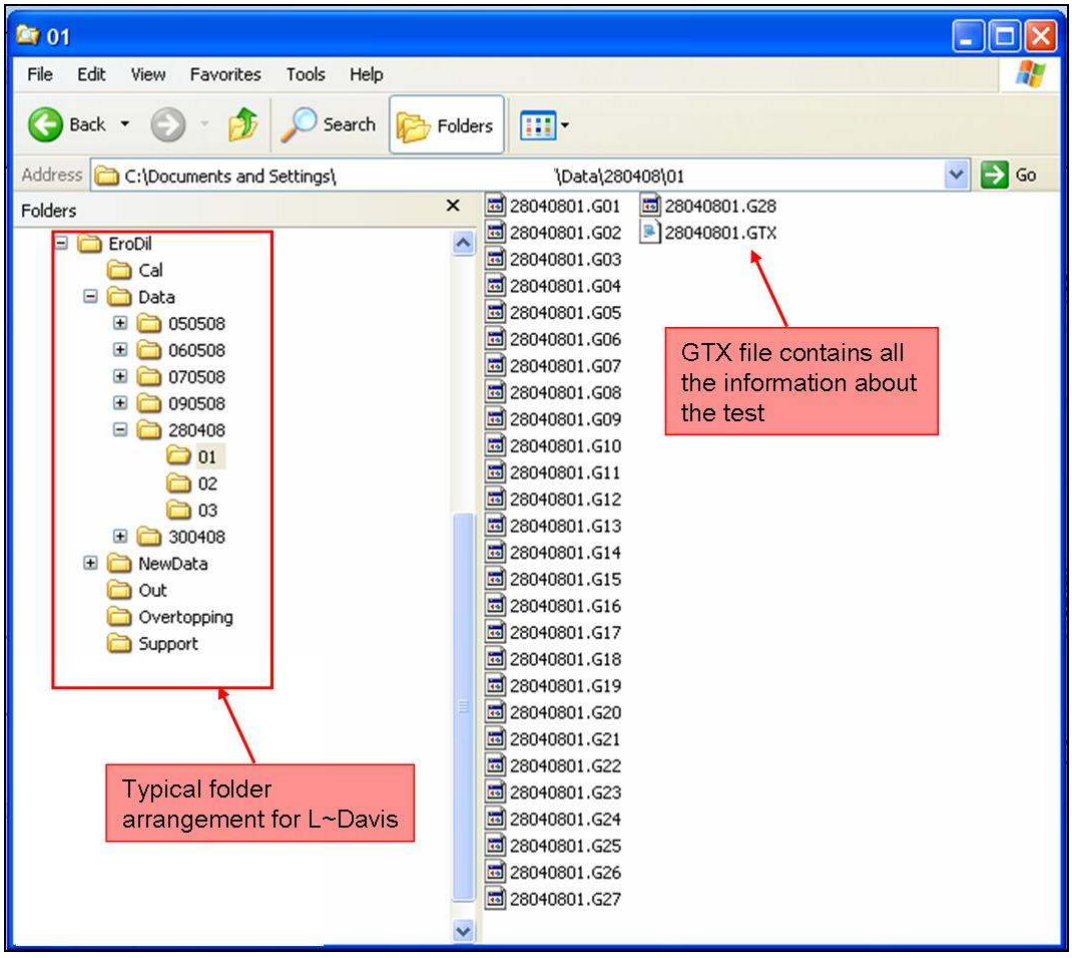

Figure A1.1 Typical folder arrangement for the data analysis with L~Davis software.

Incident waves

Three wave gauge arrays were set-up in the flume, each consisting of 4 wave gauges. 1st array was 50m from the wave maker, the second one is 84m from the wave maker and the third array was 120m from the wave maker (Figure 2.1 and Geisenhainer and Oumeraci, 2008, Page 26). Measurements from the 3rd wave gauge array are used for the reflection analysis and to find the incident wave parameter at the toe of the dike. Hm0 and Tm-1,0 are used as the characteristic parameters. All the model tests consist of approximately 1000 waves. This enables to perform statistical analysis on wave parameters. Wave data were filleted to remove the noise using frequency filtering tool provided in L~Davis software. 0.05Hz was used as high pass filter and 0.6Hz was used as low pass filter. Figure 1 gives resultant frequency spectrum using two different filters. Figure 1.1A shows the results of using 0.05Hz as high pass filter and 1.0Hz as low pass filter and the Figure 1.2 shows the results of using 0.05Hz as high pass filter and 0.6Hz as low pass filter. Wave data contains considerable amount of noises between the frequencies of 0.6Hz and 0.7Hz. Hence, it was decided to use 0.05Hz and 0.6Hz and high and low pass filters respectively.

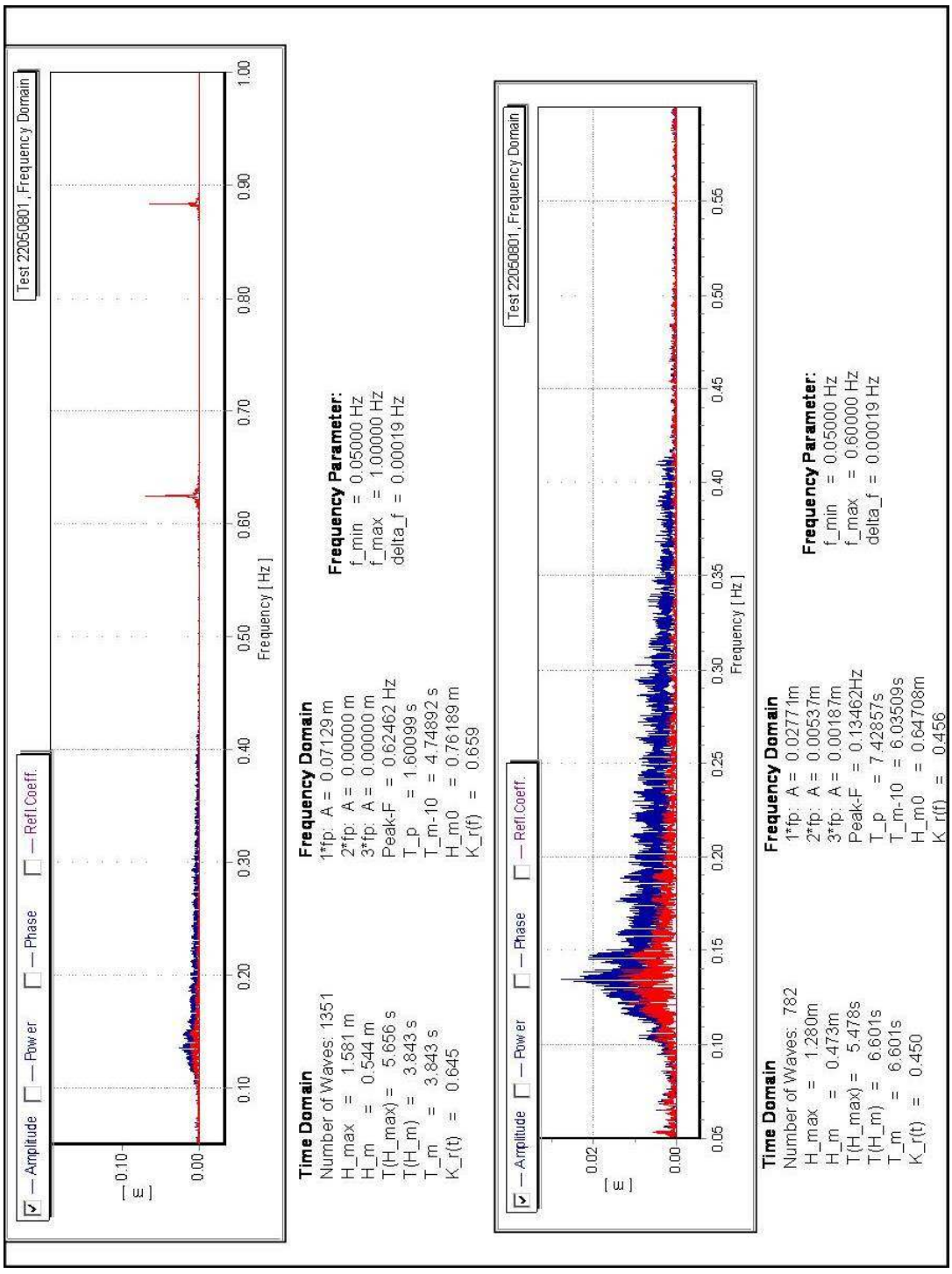

Figure A1.2 Comparison of the L~Davis outputs with different filter criterion. (nominal Wave Parameter: H = 0.7 and T = 7.500).

Table A1.1 Overview of the available data.

	APRIL																				
	Mon	Tue	Wed	Thu	Fri	Mon	Tue	Wed	Thu	Fri	Mon	Tue	Wed	Thu	Fri	Mon	Tue	Wed	Thu	Fri	Mon
Date	**7**	**8**	**9**	**10**	**11**	**14**	**15**	**16**	**17**	**18**	**21**	**22**	**23**	**24**	**25**	**28**	**29**	**30**	**1**	**2**	**5**
EroGRASS Phase 1 - seaward slope																**EroGRASS Phase 2 - landward slope**					
Wave height H_s [m]		0.8		0.8	0.9			0.5				0.7				1.0					0.75
Wave period T_p [s]		5.0		5.0	5.0			4.0				5.0				5.0					5.5
Water level d [m]		3.7		3.7	3.7			3.7				3.7				4.7					5.0
Duration of test run [s]		1800		3800	4000			4800				5100				5100					4050
Wave height H_s [m]								0.5				0.9				1.0		0.75			
Wave period T_p [s]								4.0				5.0				5.0		5.5			
Water level d [m]								3.7				3.7				4.7		5.0			
Duration of test run [s]								4800				4100				4100		4050			
Wave height H_s [m]								0.5								1.0					0.85
Wave period T_p [s]								4.0								5.0					6.0
Water level d [m]								3.7								4.7					5.0
Duration of test run [s]								4800								4100					4200
Wave height H_s [m]																					
Wave period T_p [s]																					
Water level d [m]																					
Duration of test run [s]																					
Wave height H_s [m]												0.9									
Wave period T_p [s]												5.0									
Water level d [m]												3.7									
Duration of test run [s]												4100									

Wave overtopping

Overtopping water collected by 0.21m or 0.15m wide chute at the landward edge of the dike crest and then, discharged it into an overtopping container. The overtopping container was placed on a loading cell which gives the time series of wave overtopping discharges. When the maximum possible water level was reached, the water was pumped out.

The signal of the overtopping container can be analysed to get the mean overtopping discharge and overtopping volume per wave. From these results, the mean overtopping discharge per width is calculated. Figure 1.3 shows schematic diagram of wave overtopping measuring arrangement. As shown in the figure, one weighing cell was used during the test. However, calibration factor is selected to give the total weight of the water in the overtopping collecting container.

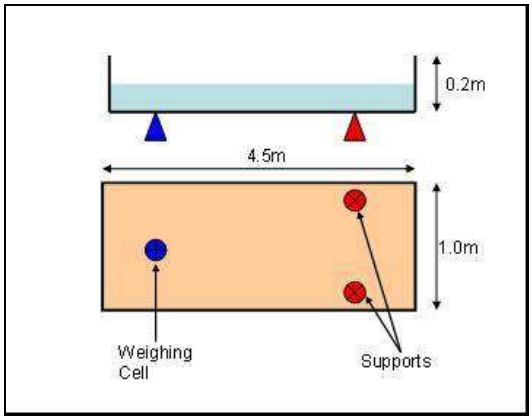

Figure A1.3 Wave overtopping arrangement

Overtopping data contain a considerable amount of noise and all the overtopping data was filtered with 2Hz low pass filter (All the signals more than the 2Hz were removed). Figure 2.5 shows a typical plot of filtered overtopping signal. Due to the limited capacity of the overtopping collecting container, collected water was pumped out during the model test (see Figure 2.5). However, the water was pumped out only when there was no overtopping. A detail description of wave overtopping data collection system is given in (Geisenhainer and Oumeraci, 2008, Page 46-47).

Flow velocity over the seaward slope of the dike

Wave run-up velocities were measured with velocimeter (mini-propellers). Due to the floating grass, propellers were frequently disturbed as expected during the planning phase of the test. Therefore, analysis of the data from the velocimeter should be done with cautious.

Pressure Measurement of the Seaward Slope of the dike

Preliminary analysis of pressure data was done under the FLOODsite project and detail analysis is still going on at LWI.

A2 Results

This section describes the results from the preliminary data analysis of the model tests. Measured wave parameters were compared with nominal wave parameters, which were given as the inputs to the wave maker and overtopping results were compared with the formulae given in EurOtop (2007). Only the data from the test phase 2 was used for preliminary analysis.

Incident wave parameters at the toe of the dike

All the calculations were done based on the incident wave parameter at the toe of the dike. 3rd wave gauge array (see Figure A2.1) was used to perform reflection analysis and to find the incident wave height and time periods at the toe of the dike.

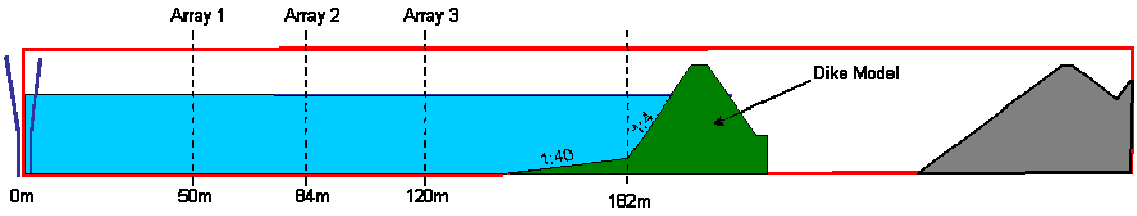

Figure A2.1 Locations of wave gauge arrays

Figure A2.2 shows the methodology followed during the preliminary analysis of incident wave parameter in front of the dike.

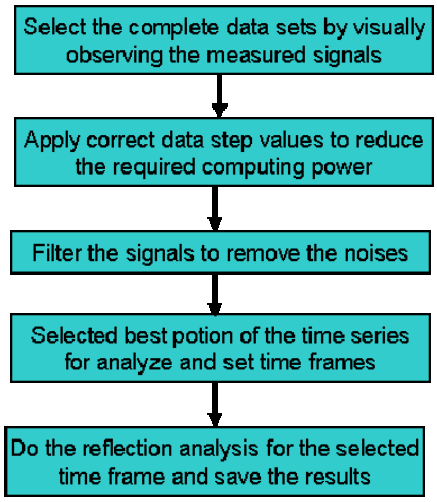

Figure A2.2 Methodology followed during preliminary data analysis

Results from the wave analysis

Incident wave parameters during the test phase 2 are plotted in Figure 2.3 and Figure 2.4. As shown in Figure 2.3, the incident wave heights are 0% to 10% lower than the nominal values. Also, the wave period, $T_{m0,-1}$ is 10% to 20% lower than the nominal T_p value. Data from the test on 08th of April, 2008 shows a clear deviation from the general trend.

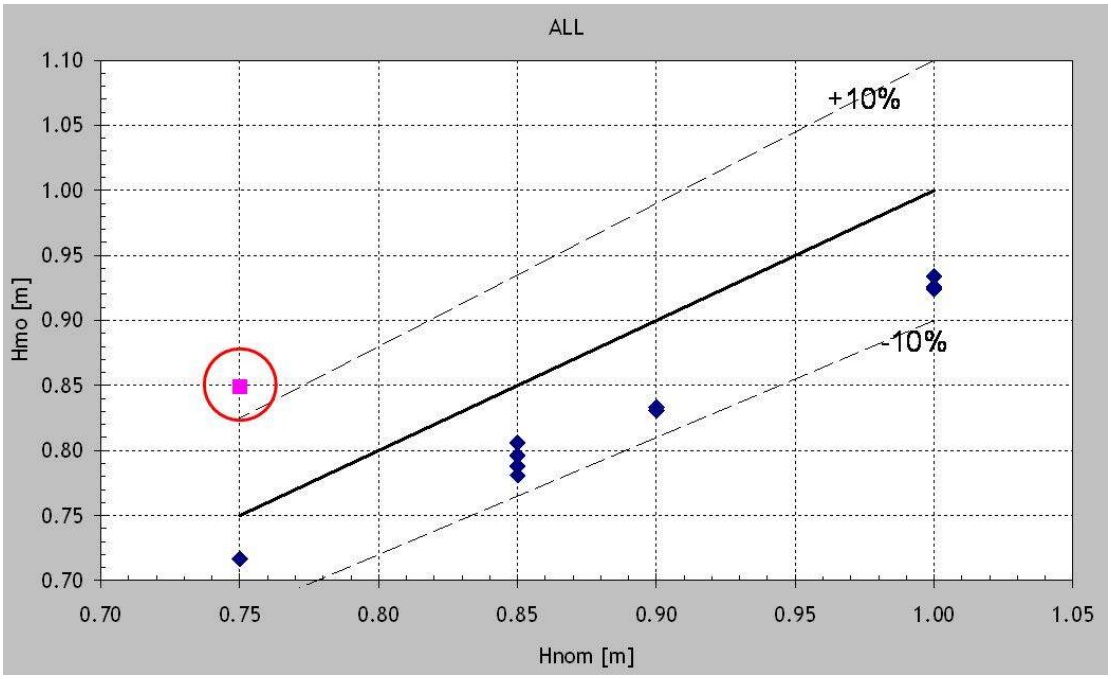

Figure A2.3 Measured wave height during the test phase 2.

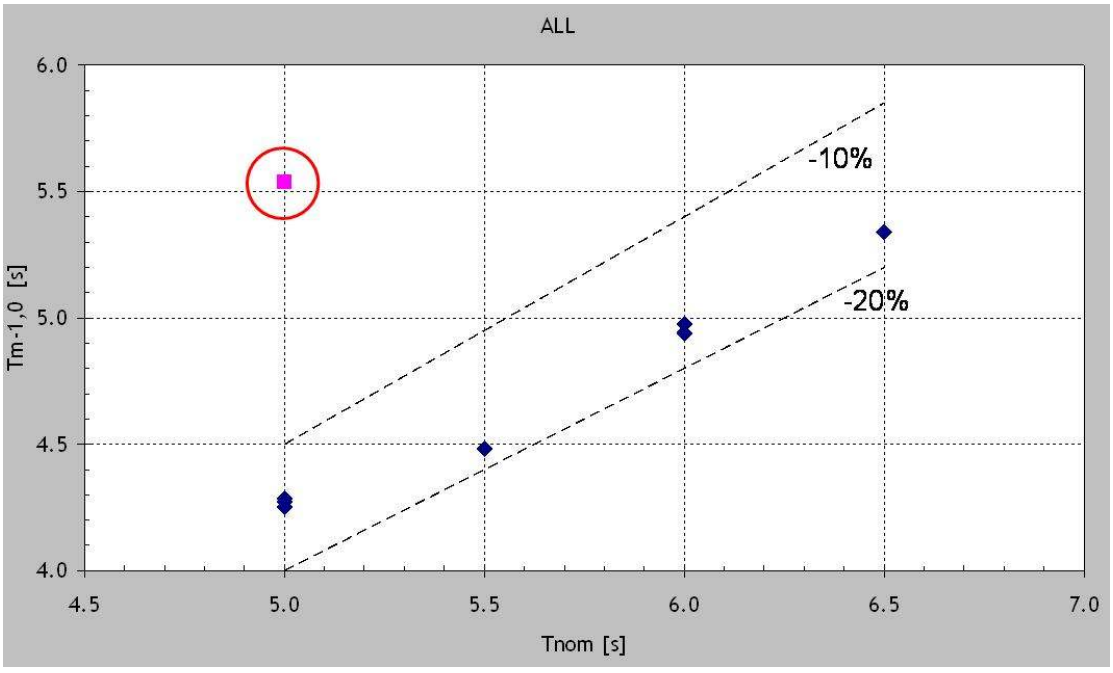

Figure A2.4 Measured wave periods during the test phase 2.

Mean overtopping discharge

Mean overtopping discharges were calculated summing all the filling time series and dividing it over the entire period of the test. Pumping was carried out when there is not overtopping. As number of pumping events are higher, the event analysis tool of the L-Davis software was used to find the pumping event (see figure 2.5). All the selected events were checked with the manual records of pumping events. Then, each overtopping event were summed and divided by total duration of the test to find the mean overtopping discharge.

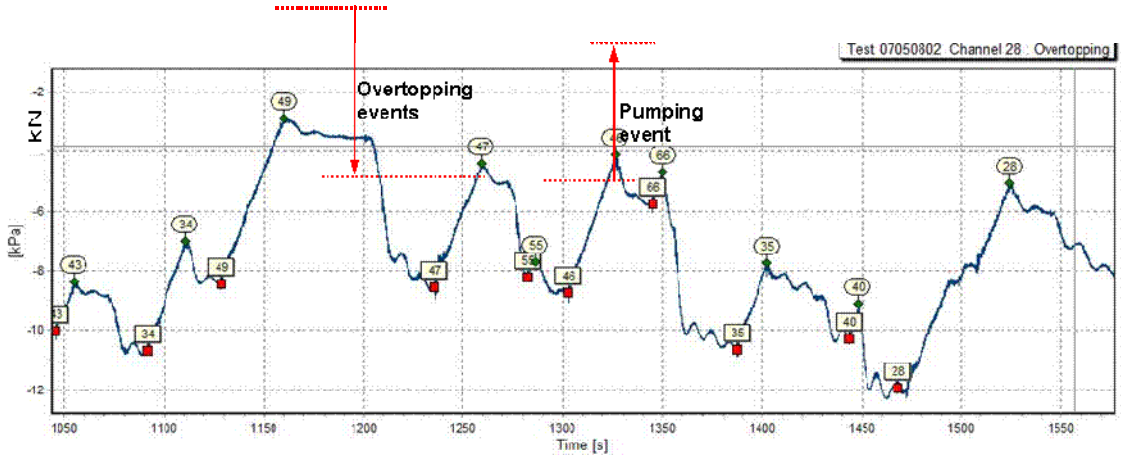

Figure A2.5 Typical overtopping record (Nominal Wave Parameter: H = 0.85m and T = 6.0s).

The mean overtopping discharges were compared with the formulae given in EurOtop (2007). Figure 2.6 shows the preliminary results from the overtopping analysis. The mean overtopping discharges measurements show a reasonable agreement with the guidelines provided by EurOtop (2007).

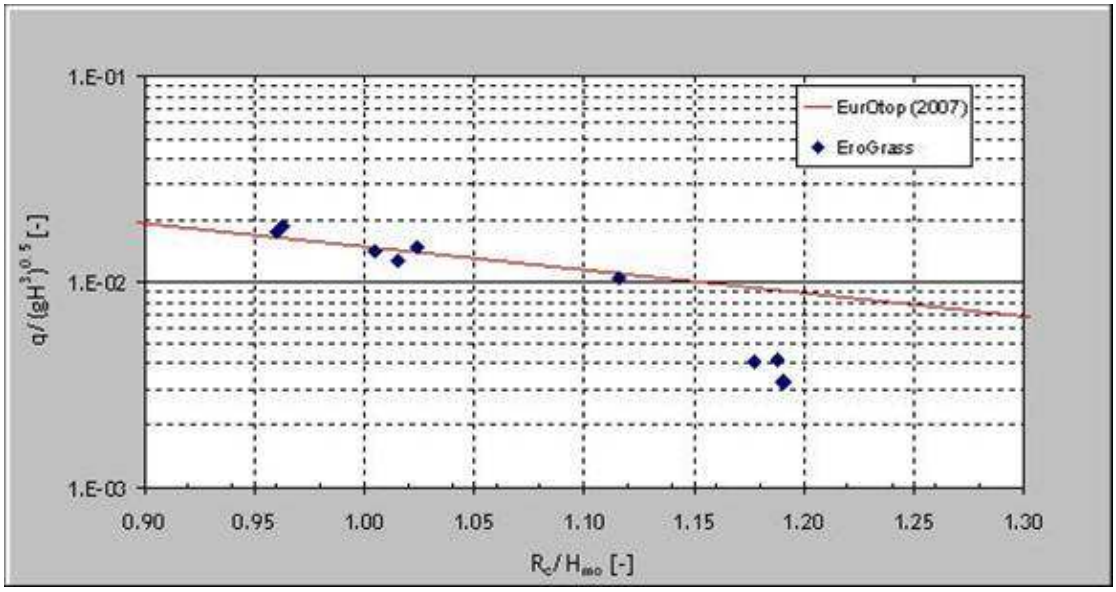

Figure A2.6 Mean overtopping discharge measurements.

A3 Conclusions and Recommendations

The results from the preliminary data analyses show a reasonable agreement between the expected results in incident wave parameters in front of the dike and mean overtopping discharges and the measured values. Overtopping volume per wave can be found from the time series data of wave overtopping measurements. However, the results should cross check with the manual pumping records as well as videos.

The analysis of the data from the velocimeter should be done with cautious and the video records can be analysed to find velocities over the surface of the dike with reference the grid drawn on the internal walls of the flume.

Finally, it is recommended to use the L~Davis, data analysis and visualisation software developed by LWI for the detail analysis of data since it fully support the format of acquired data as well as L~Davis gives number of possibilities to control the equality of the output.

References

EurOtop 2007. European Overtopping Manual. Eds Pullen, T.; Allsop, N.W.H.; Bruce, T.; Kortenhaus, A.; Schüttrumpf, H.; Van der Meer, J.W.; www.overtopping-manual.com.

Geisenhainer P. and Oumeraci, H. (2008), Report Sea dike breach initiation and development-Large Scale Experiments In GWK, Report Number T06-08-12, FLOODsite-Integrated Flood Risk Assessment and Management Methodologies, Task 6, Braunschweig, Germany.

http://www.lwi.tu-bs.de/hyku/english/en_Ldavis-index.html

Appendix B: Data storage plan

Xxx

Appendix C: User group

Danish Coastal Authority
Hoebovej 1
7620 Lemvig
Denmark
Thorsten Piontkowitz
Project Management EroGRASS
E-mail: tpi@kyst.dk
Phone: +45 99 63 63 24
Fax: +45 99 63 63 99

UNESCO-IHE Institute for Water Education
Westvest 7
P.O. Box 3015
2601 DA Delft
The Netherlands
Prof. Dano Roelvink
E-mail: d.roelvink@unesco-ihe.org
Phone: +31 (15) 21 51 838
Fax: +31 (15) 21 22 921

Delft University of Technology
Hydraulic Engineering Section
Stevinweg 1
P.O. Box 5048
NL-2600 GA Delft
The Netherlands
Henk Jan Verhagen
E-mail: h.j.verhagen@tudelft.nl
Phone: +31 (15) 278 5067
Fax: +31 (15) 278 5124

Deltares | Delft Hydraulics
Rotterdamseweg 185
P.O. Box 177
2600 MH Delft
The Netherlands
Henk Verheij
E-mail: henk.verheij@deltares.nl
Phone: +31 (15) 285 87 37
Fax: +31 (15) 285 85 82

University of Strathclyde
Department of Civil Engineering
John Anderson Building
107 Rottenrow
Glasgow G4 ONG
UK
Stefano Utili
E-mail: stefano.utili@strath.ac.uk
Phone: +44 (0) 141 548 3277
Fax: +44 (0) 141 553 2066

Marcin Zielinski
E-mail: marcin.zielinski@strath.ac.uk
Phone: +44 (0) 141 548 3161
Fax: +44 (0) 141 553 2066

Tallinn University
Department of Natural Sciences
Chair of Biology
Narva mnt. 25
10120 Tallinn
Estonia
Tõnu Ploompuu
E-mail: toenu@tlu.ee
Phone: +372 (6409) 416
Fax: +372 (6409) 418

Institute of Ecology
Uus-Sadama 5
10120 Tallinn
Estonia
Are Kont
E-mail: are@tlu.ee
Phone: +372 (619) 9800
Fax: +372 (619) 9801